**Supplementary Materials**

# Exploring structures of nanoclusters combining high-dimensional neural network potentials with unsupervised machine learning algorithms

**Huabing Cai[1], Aoni Xu[2], Dan Villamanca[2], Ang Cao[1,3], Jianhua Yan[1]**

[1]State Key Laboratory of Clean Energy Utilization, College of Energy Engineering, Zhejiang University, Hangzhou 310027, Zhejiang, China.
[2]School of Chemical and Biomolecular Engineering, The University of Sydney, Sydney 2006, Australia.
[3]Mongolia Daqingshan Laboratory, Hohhot 017000, Inner Mongolia, China.

**Correspondence to:** Dr. Ang Cao, State Key Laboratory of Clean Energy Utilization, College of Energy Engineering, Zhejiang University, Hangzhou 310027, Zhejiang, China; Mongolia Daqingshan Laboratory, Hohhot 017000, Inner Mongolia, China. E-mail: angc@zju.edu.cn

## 1. The high-dimensional neural network[1, 2]

The main idea of this neural network is to represent the total energy as the sum of the energies of all the atoms,

$$E = \sum_i E_i \tag{1}$$

The $E_i$ represents the energy of atom $i$. The atomic energies are trained by atomic neural networks using the symmetry functions to describe each atom's structural and chemical environment information. In this work, we choose the following three symmetry functions to represent the local chemical environment of all the atoms (oxygen, cerium atoms) from Cartesian coordinates, and the mathematical expressions of the three symmetry functions are as follows:

Radial symmetry function

$$G_i^{radial} = \sum_{j \neq i} e^{-\eta (r_{ij} - r_s)^2} f_c(r_{ij}) \quad (2)$$

Narrow angular symmetry function

$$G_i^{ang.n.} = 2^{1-\zeta} \sum_{\substack{j,k \neq i \\ j<k}} (1 + \lambda \cos\theta_{ijk})^{\zeta} e^{-\eta\left((r_{ij} - r_s)^2 + (r_{ik} - r_s)^2 + (r_{jk} - r_s)^2\right)} f_c(r_{ij}) f_c(r_{ik}) f_c(r_{jk}) \quad (3)$$

Wide angular symmetry function

$$G_i^{ang.w.} = 2^{1-\zeta} \sum_{\substack{j,k \neq i \\ j<k}} (1 + \lambda \cos\theta_{ijk})^{\zeta} e^{-\eta\left((r_{ij} - r_s)^2 + (r_{ik} - r_s)^2\right)} f_c(r_{ij}) f_c(r_{ik}) \quad (4)$$

And, $f_c(r_{ij})$ represents the cutoff function, which has the form

$$f_c(r_{ij}) = \begin{cases} 0.5 \times \left[\cos\left(\frac{\pi r_{ij}}{r_c}\right) + 1\right] & \text{for } r_{ij \leq} r_c, \\ 0 & \text{for } r_{ij >} r_c. \end{cases} \quad (5)$$

$r_{ij}$ represents the distance between atom $i$ and atom $j$. $r_c$ represents the cutoff radius.

To evaluate the accuracy of the neural network potential (NNP), the root-mean-square error (RMSE) of energies calculated by DFT and predicted by NNP is defined as:

$$RMSE = \sqrt{\frac{1}{M} \sum_{i=1}^{M} \left(E_{DFT}^{ref} - E_{NNP}\right)^2} \quad (6)$$

$M$ represents the total number of data sets.

**Supplementary Table 1.** Parameters of symmetry functions performed using the n2p2 code[3]

| Radial | | | Angular | | | | |
|---|---|---|---|---|---|---|---|
| $\eta$ | $r_s$ | $r_c$ | $\eta$ | $\lambda$ | $\zeta$ | $r_s$ | $r_c$ |
| 2 | 1.5 | 6 | 0.2222 | -1 | 1 | 0 | 6 |
| 2 | 2 | 6 | 0.2222 | 1 | 1 | 0 | 6 |
| 2 | 2.5 | 6 | 0.2222 | -1 | 6 | 0 | 6 |
| 2 | 3 | 6 | 0.2222 | 1 | 6 | 0 | 6 |
| 2 | 3.5 | 6 | 0.0408 | -1 | 1 | 0 | 6 |
| 2 | 4 | 6 | 0.0408 | 1 | 1 | 0 | 6 |
| 2 | 4.5 | 6 | 0.0408 | -1 | 6 | 0 | 6 |
| 2 | 5 | 6 | 0.0408 | 1 | 6 | 0 | 6 |
| 2 | 5.5 | 6 | 0.0165 | -1 | 1 | 0 | 6 |
| | | | 0.0165 | 1 | 1 | 0 | 6 |
| | | | 0.0165 | -1 | 6 | 0 | 6 |
| | | | 0.0165 | 1 | 6 | 0 | 6 |

## 2. The low-energy structures of cerium oxide nanoclusters

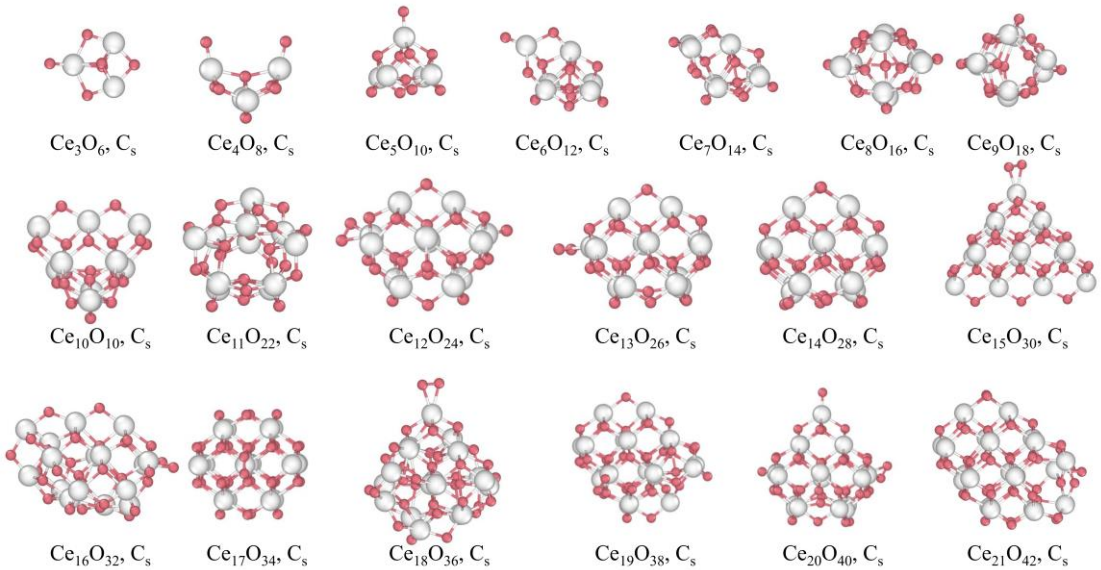

**Supplementary Figure 1.** The most stable structures and their corresponding symmetries of stoichiometric cerium oxide clusters ranging from $Ce_3O_6$ to $Ce_{21}O_{42}$. Color code: red, O atom; white, Ce atom.

**Supplementary Table 2.** Comparison of NNP-predicted energies and DFT-calculated energies for the lowest-energy structures

| Nanoclusters | NNP-predicted energy (eV ) | DFT-calculated energy (eV) | Absolute energy errors (eV) |
|---|---|---|---|
| Ce3O6 | -64.094 | -63.935 | 0.158 |
| Ce4O8 | -87.013 | -86.995 | 0.018 |
| Ce5O10 | -110.283 | -110.179 | 0.104 |
| Ce6O12 | -133.252 | -133.179 | 0.073 |
| Ce7O14 | -156.483 | -156.440 | 0.043 |
| Ce8O16 | -179.879 | -180.062 | 0.183 |
| Ce9O18 | -203.045 | -203.242 | 0.197 |
| Ce10O20 | -226.315 | -226.679 | 0.364 |
| Ce11O22 | -249.062 | -249.194 | 0.128 |
| Ce12O24 | -272.963 | -273.062 | 0.099 |
| Ce13O26 | -296.164 | -296.598 | 0.434 |
| Ce14O28 | -320.855 | -320.756 | 0.099 |
| Ce15O30 | -343.747 | -343.661 | 0.086 |
| Ce16O32 | -366.086 | -366.354 | 0.268 |
| Ce17O34 | -388.722 | -388.977 | 0.255 |
| Ce18O36 | -412.740 | -412.807 | 0.067 |
| Ce19O38 | -436.624 | -437.019 | 0.395 |
| Ce20O40 | -461.206 | -461.373 | 0.167 |
| Ce21O42 | -484.147 | -484.490 | 0.343 |

The stability function was defined as follows:

$$\Delta^2 E(Ce_nO_{2n}) = 2E_{tot}^{Ce_nO_{2n}} - E_{tot}^{Ce_{(n-1)}O_{2(n-1)}} - E_{tot}^{Ce_{(n+1)}O_{2(n+1)}} \qquad (7)$$

Wherein the range of n is from 4 to 20, and $E_{tot}^{Ce_nO_{2n}}$ denotes the total energy of the cluster $Ce_nO_{2n}$.

## 3. The NNPMD simulations of the most stable nanoclusters

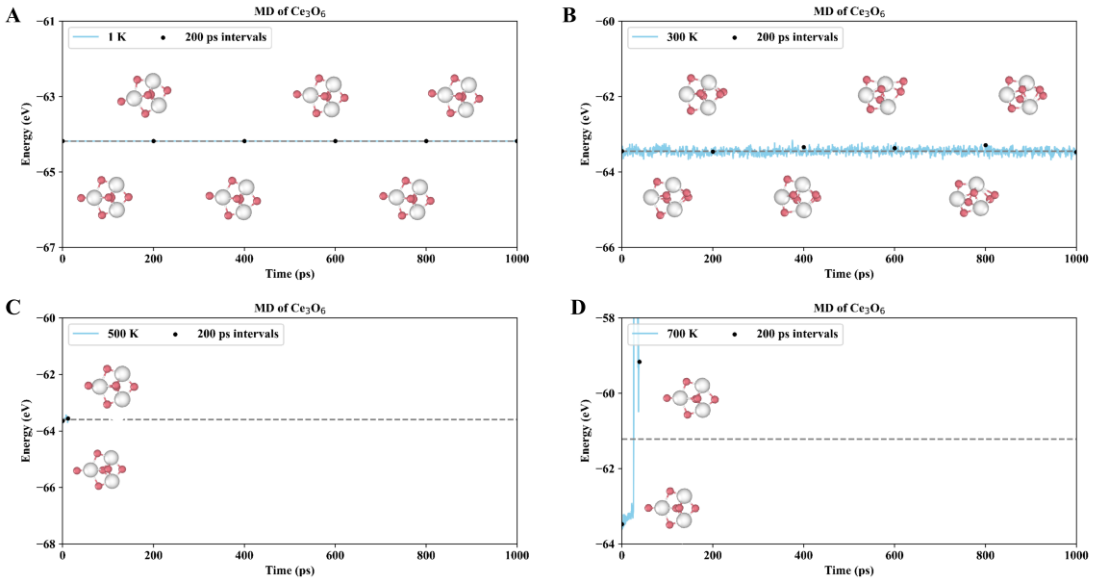


**Supplementary Figure 2.** Molecular dynamics (MD) simulations of the most stable cerium oxide nanocluster $Ce_3O_6$ at different temperatures, including energies during the simulations and snapshots taken every 200 ps. A: 1 K; B: 300 K; C: 500 K; D: 700 K. Color map: white, Ce atoms; pink, O atoms.

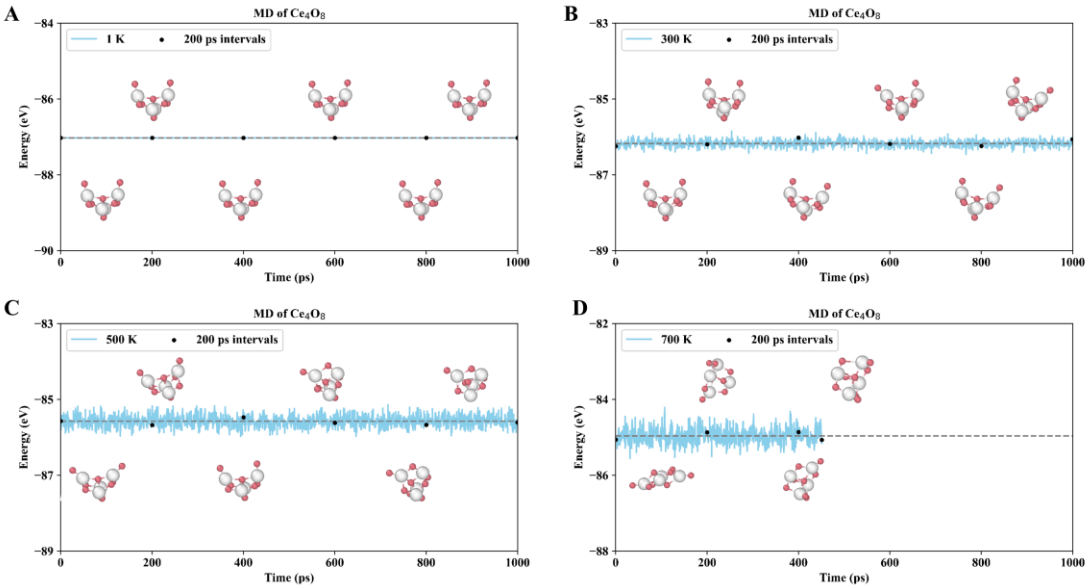


**Supplementary Figure 3.** Molecular dynamics (MD) simulations of the most stable cerium oxide nanocluster $Ce_4O_8$ at different temperatures, including energies during the simulations and snapshots taken every 200 ps. A: 1 K; B: 300 K; C: 500 K; D: 700 K. Color map: white, Ce atoms; pink, O atoms.

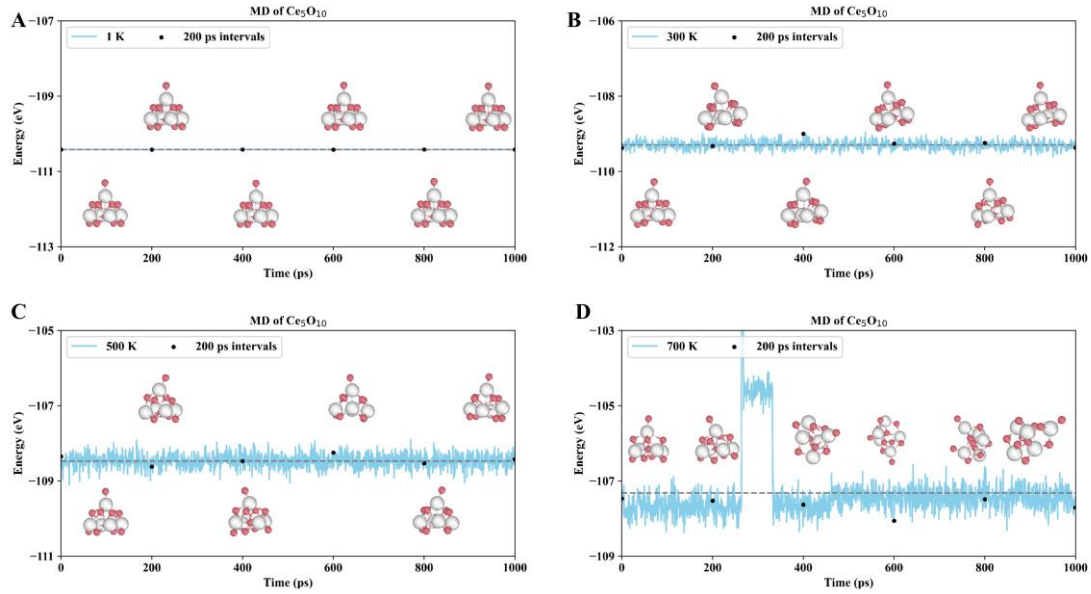


**Supplementary Figure 4.** Molecular dynamics (MD) simulations of the most stable cerium oxide nanocluster $Ce_5O_{10}$ at different temperatures, including energies during the simulations and snapshots taken every 200 ps. A: 1 K; B: 300 K; C: 500 K; D: 700 K. Color map: white, Ce atoms; pink, O atoms.

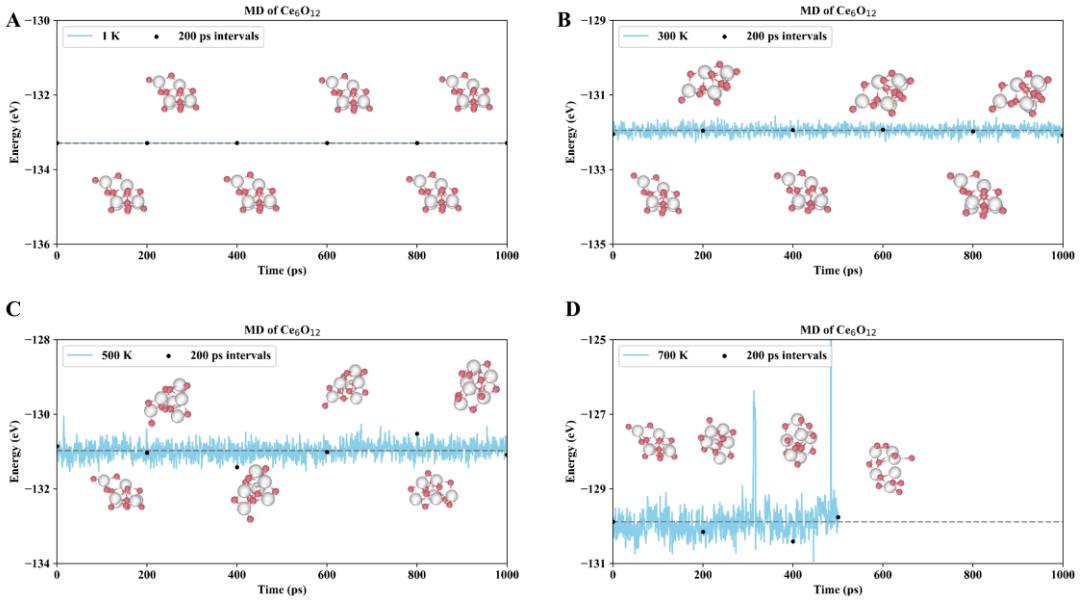


**Supplementary Figure 5.** Molecular dynamics (MD) simulations of the most stable cerium oxide nanocluster $Ce_6O_{12}$ at different temperatures, including energies during the simulations and snapshots taken every 200 ps. A: 1 K; B: 300 K; C: 500 K; D: 700 K. Color map: white, Ce atoms; pink, O atoms.

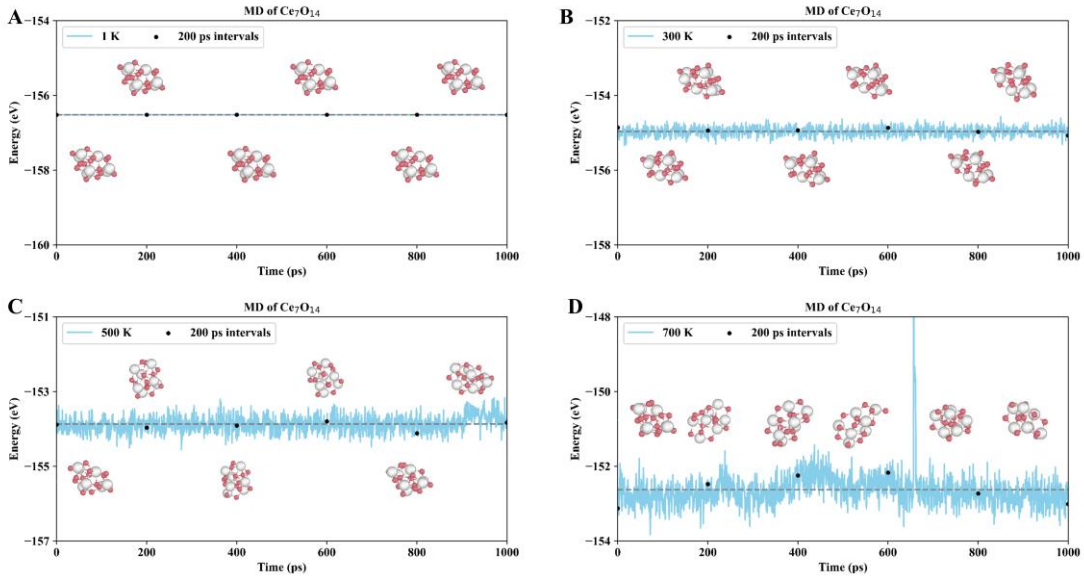


**Supplementary Figure 6.** Molecular dynamics (MD) simulations of the most stable cerium oxide nanocluster $Ce_7O_{14}$ at different temperatures, including energies during the simulations and snapshots taken every 200 ps. A: 1 K; B: 300 K; C: 500 K; D: 700 K. Color map: white, Ce atoms; pink, O atoms.

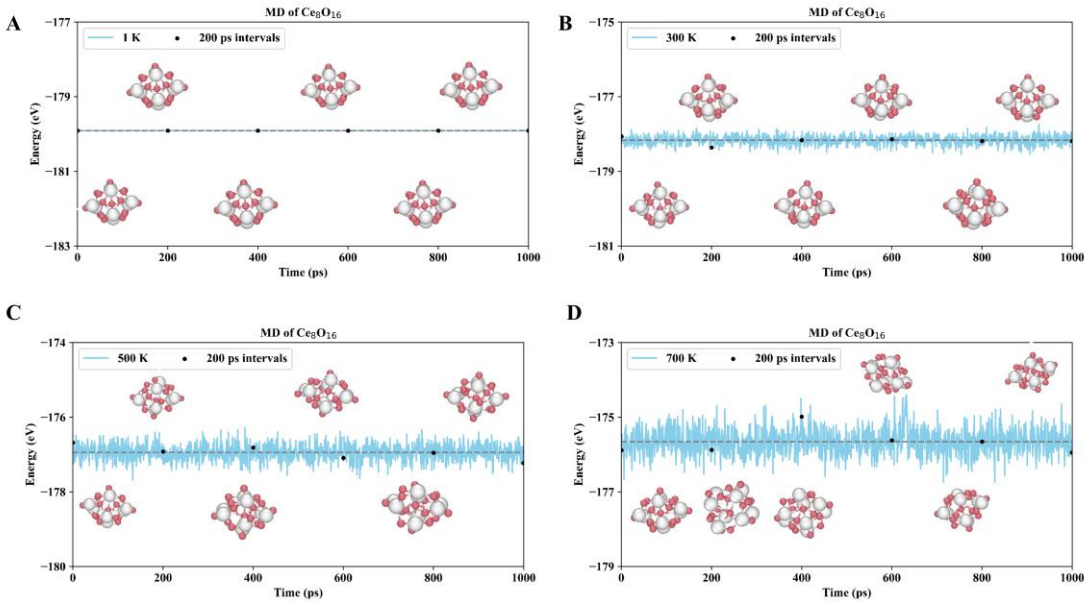


**Supplementary Figure 7.** Molecular dynamics (MD) simulations of the most stable cerium oxide nanocluster $Ce_8O_{16}$ at different temperatures, including energies during the simulations and snapshots taken every 200 ps. A: 1 K; B: 300 K; C: 500 K; D: 700 K. Color map: white, Ce atoms; pink, O atoms.

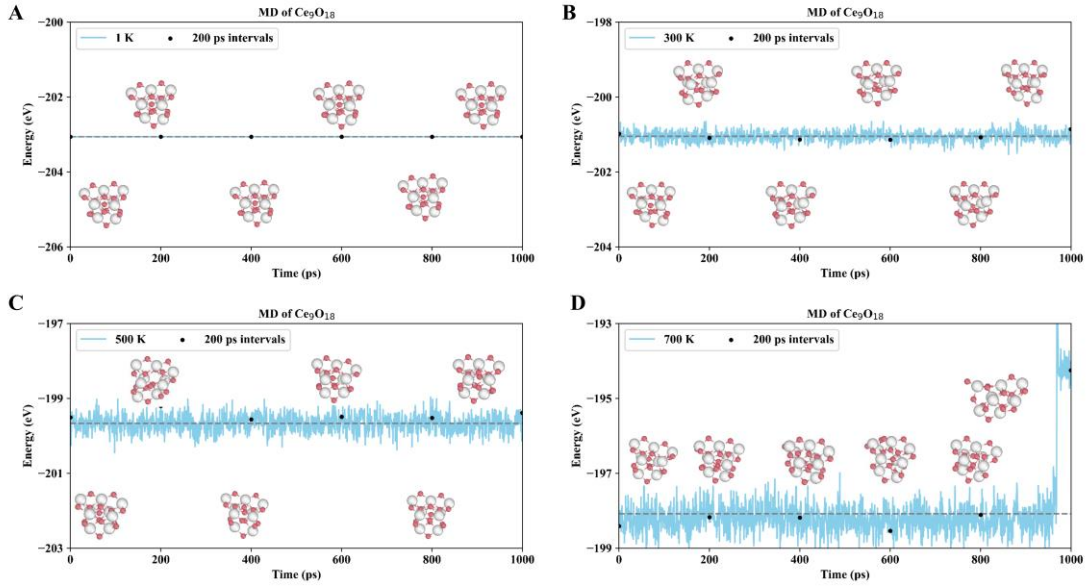


**Supplementary Figure 8.** Molecular dynamics (MD) simulations of the most stable cerium oxide nanocluster $Ce_9O_{18}$ at different temperatures, including energies during the simulations and snapshots taken every 200 ps. A: 1 K; B: 300 K; C: 500 K; D: 700 K. Color map: white, Ce atoms; pink, O atoms.

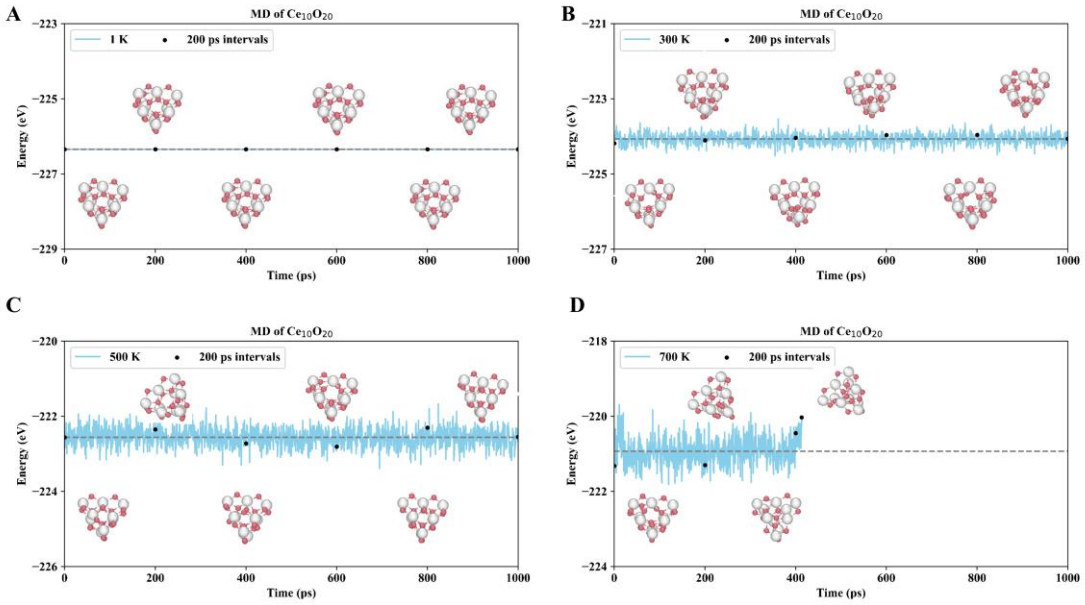


**Supplementary Figure 9.** Molecular dynamics (MD) simulations of the most stable cerium oxide nanocluster $Ce_{10}O_{20}$ at different temperatures, including energies during the simulations and snapshots taken every 200 ps. A: 1 K; B: 300 K; C: 500 K; D: 700 K. Color map: white, Ce atoms; pink, O atoms.

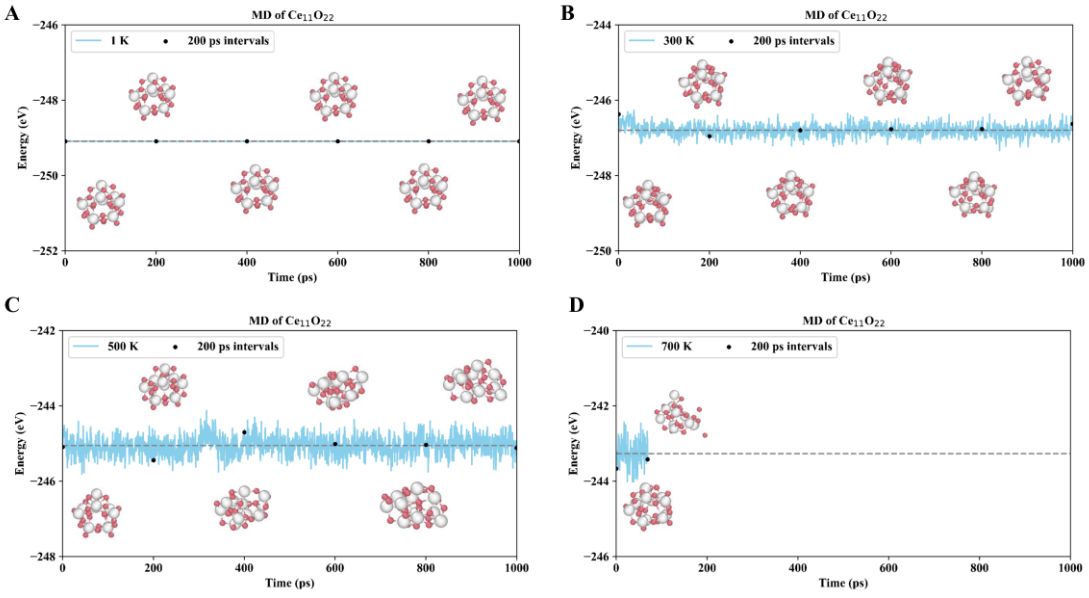


**Supplementary Figure 10.** Molecular dynamics (MD) simulations of the most stable cerium oxide nanocluster $Ce_{11}O_{22}$ at different temperatures, including energies during the simulations and snapshots taken every 200 ps. A: 1 K; B: 300 K; C: 500 K; D: 700 K. Color map: white, Ce atoms; pink, O atoms.

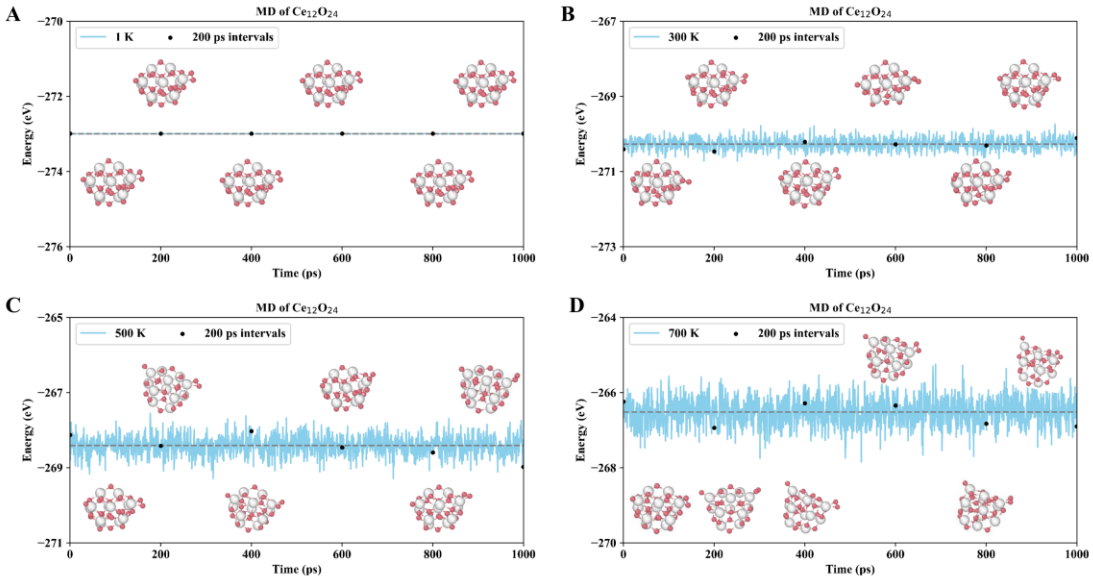


**Supplementary Figure 11.** Molecular dynamics (MD) simulations of the most stable cerium oxide nanocluster $Ce_{12}O_{24}$ at different temperatures, including energies during the simulations and snapshots taken every 200 ps. A: 1 K; B: 300 K; C: 500 K; D: 700 K. Color map: white, Ce atoms; pink, O atoms.

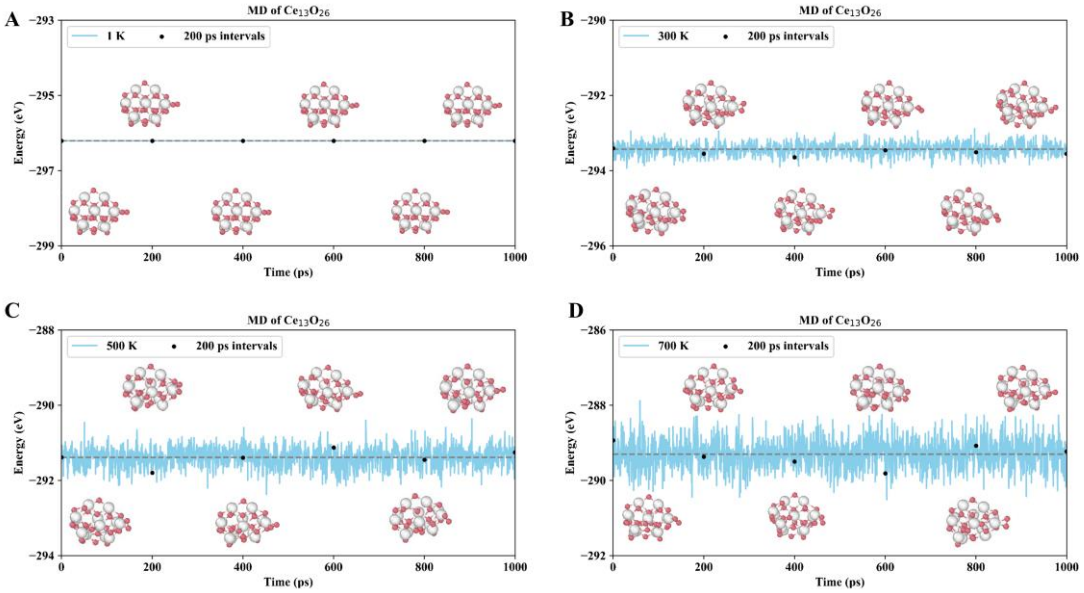


**Supplementary Figure 12.** Molecular dynamics (MD) simulations of the most stable cerium oxide nanocluster $Ce_{13}O_{26}$ at different temperatures, including energies during the simulations and snapshots taken every 200 ps. A: 1 K; B: 300 K; C: 500 K; D: 700 K. Color map: white, Ce atoms; pink, O atoms.

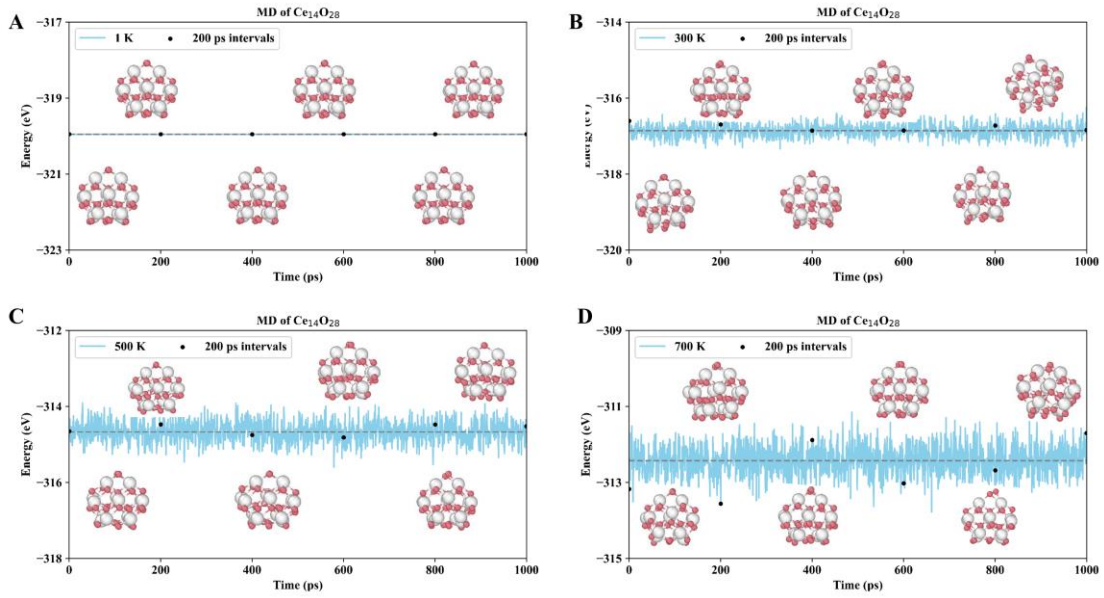


**Supplementary Figure 13.** Molecular dynamics (MD) simulations of the most stable cerium oxide nanocluster $Ce_{14}O_{28}$ at different temperatures, including energies during the simulations and snapshots taken every 200 ps. A: 1 K; B: 300 K; C: 500 K; D: 700 K. Color map: white, Ce atoms; pink, O atoms.

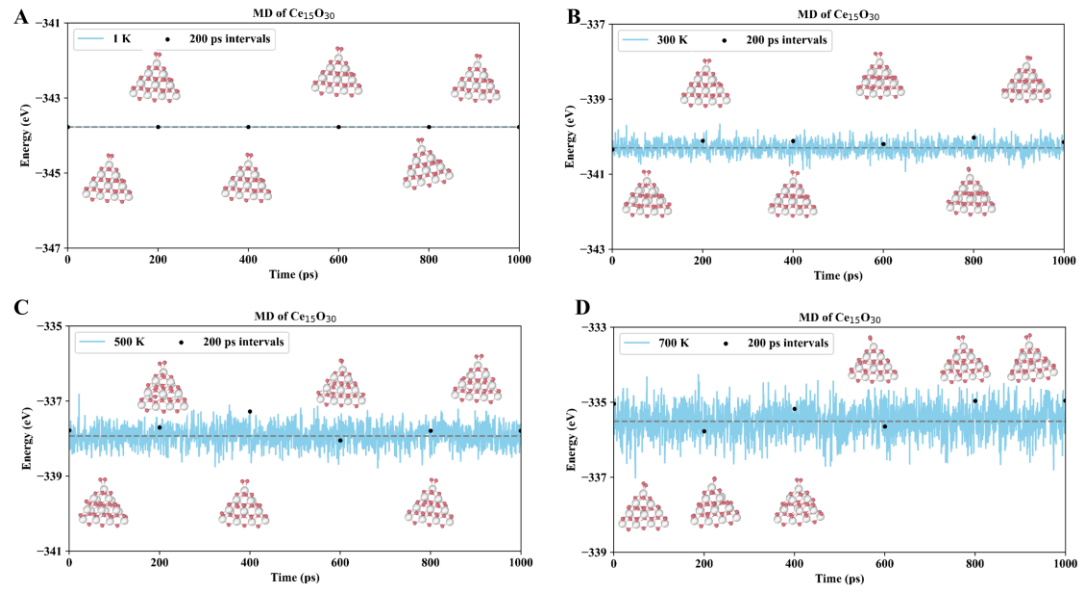


**Supplementary Figure 14.** Molecular dynamics (MD) simulations of the most stable cerium oxide nanocluster $Ce_{15}O_{30}$ at different temperatures, including energies during the simulations and snapshots taken every 200 ps. A: 1 K; B: 300 K; C: 500 K; D: 700 K. Color map: white, Ce atoms; pink, O atoms.

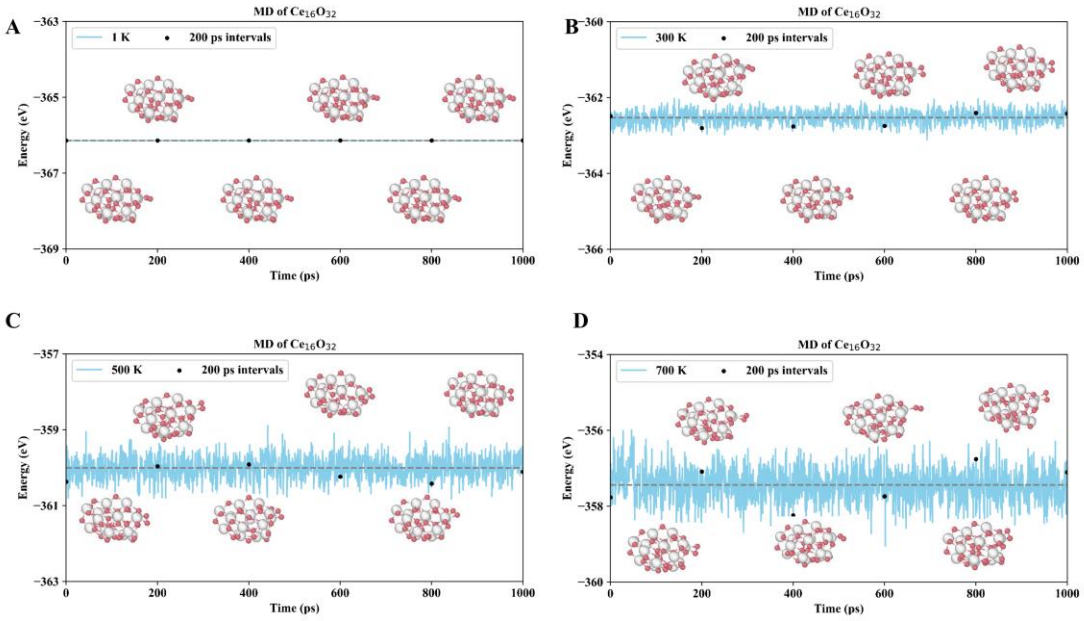


**Supplementary Figure 15.** Molecular dynamics (MD) simulations of the most stable cerium oxide nanocluster $Ce_{16}O_{32}$ at different temperatures, including energies during the simulations and snapshots taken every 200 ps. A: 1 K; B: 300 K; C: 500 K; D: 700 K. Color map: white, Ce atoms; pink, O atoms.

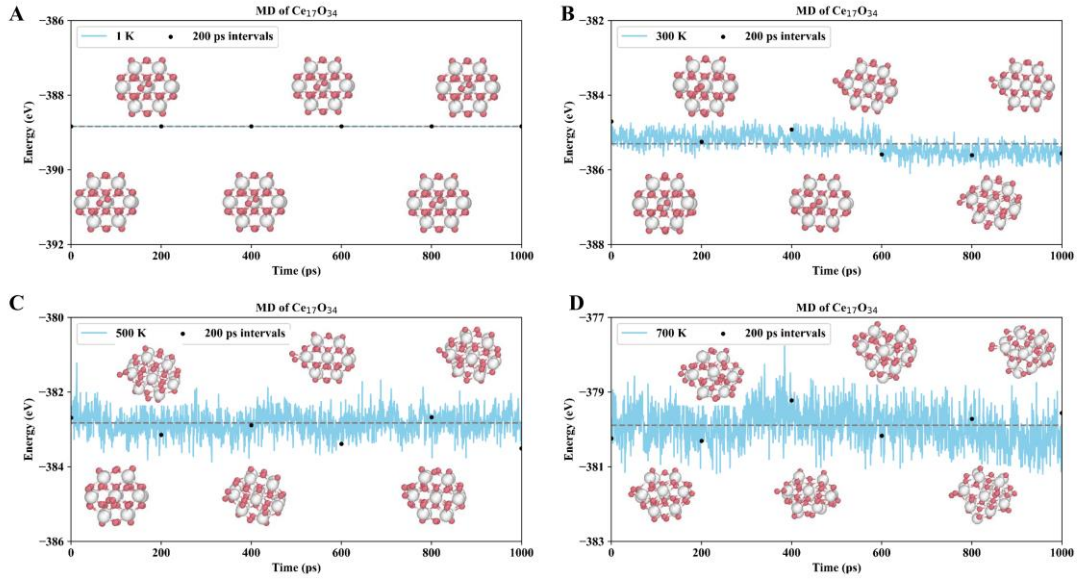


**Supplementary Figure 16.** Molecular dynamics (MD) simulations of the most stable cerium oxide nanocluster $Ce_{17}O_{34}$ at different temperatures, including energies during the simulations and snapshots taken every 200 ps. A: 1 K; B: 300 K; C: 500 K; D: 700 K. Color map: white, Ce atoms; pink, O atoms.

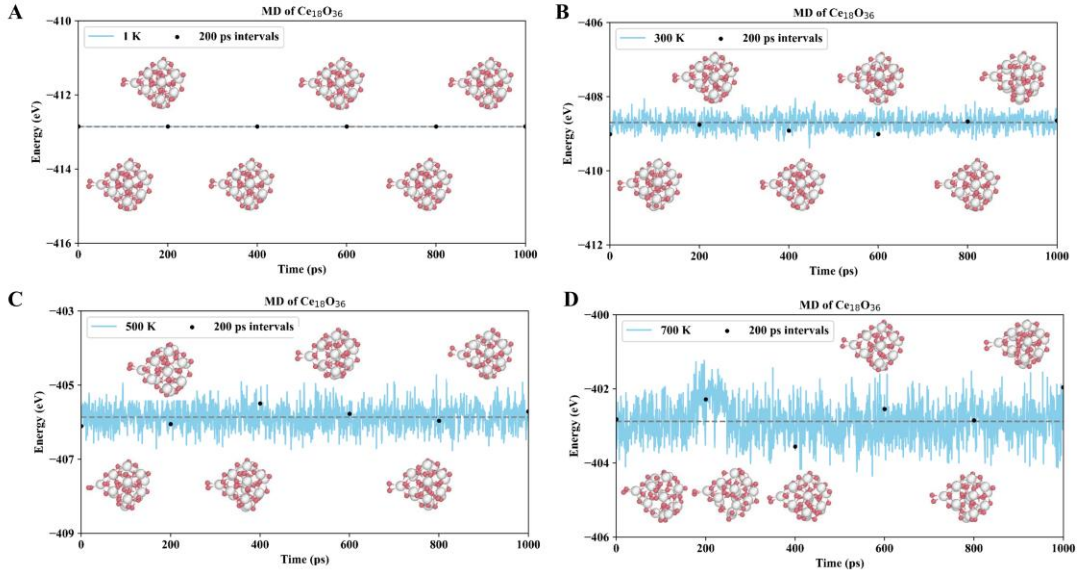


**Supplementary Figure 17.** Molecular dynamics (MD) simulations of the most stable cerium oxide nanocluster $Ce_{18}O_{36}$ at different temperatures, including energies during the simulations and snapshots taken every 200 ps. A: 1 K; B: 300 K; C: 500 K; D: 700 K. Color map: white, Ce atoms; pink, O atoms.

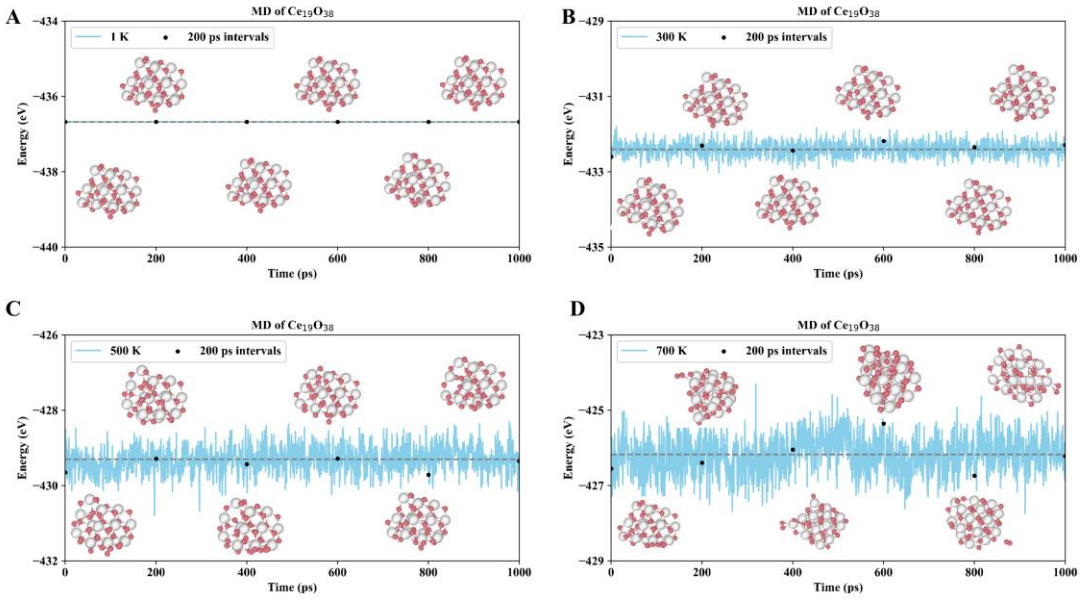


**Supplementary Figure 18.** Molecular dynamics (MD) simulations of the most stable cerium oxide nanocluster $Ce_{19}O_{38}$ at different temperatures, including energies during the simulations and snapshots taken every 200 ps. A: 1 K; B: 300 K; C: 500 K; D: 700 K. Color map: white, Ce atoms; pink, O atoms.

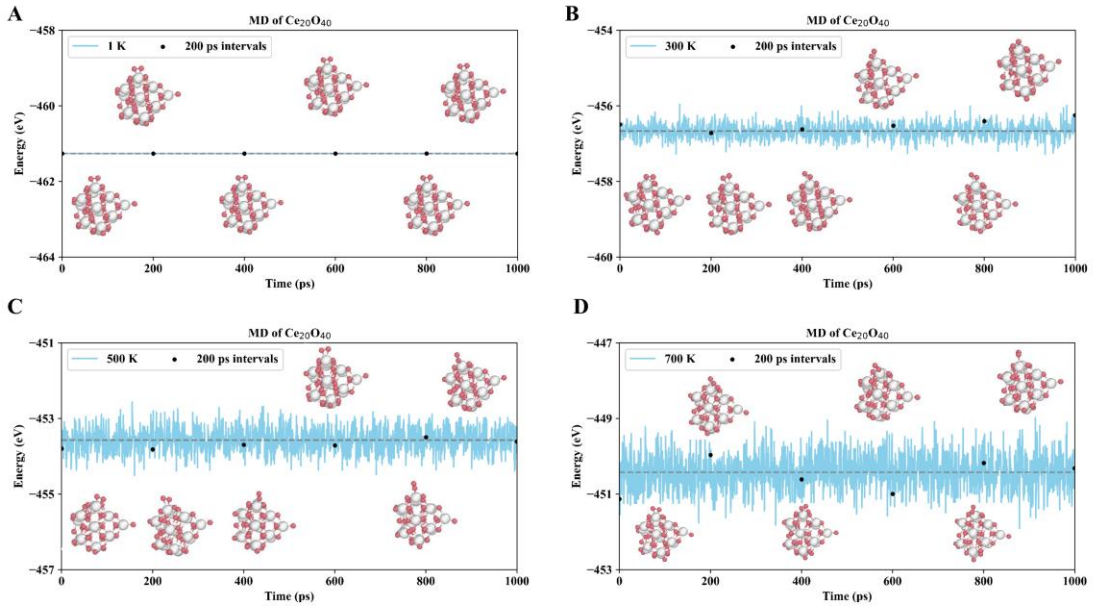


**Supplementary Figure 19.** Molecular dynamics (MD) simulations of the most stable cerium oxide nanocluster $Ce_{20}O_{40}$ at different temperatures, including energies during the simulations and snapshots taken every 200 ps. A: 1 K; B: 300 K; C: 500 K; D: 700 K. Color map: white, Ce atoms; pink, O atoms.

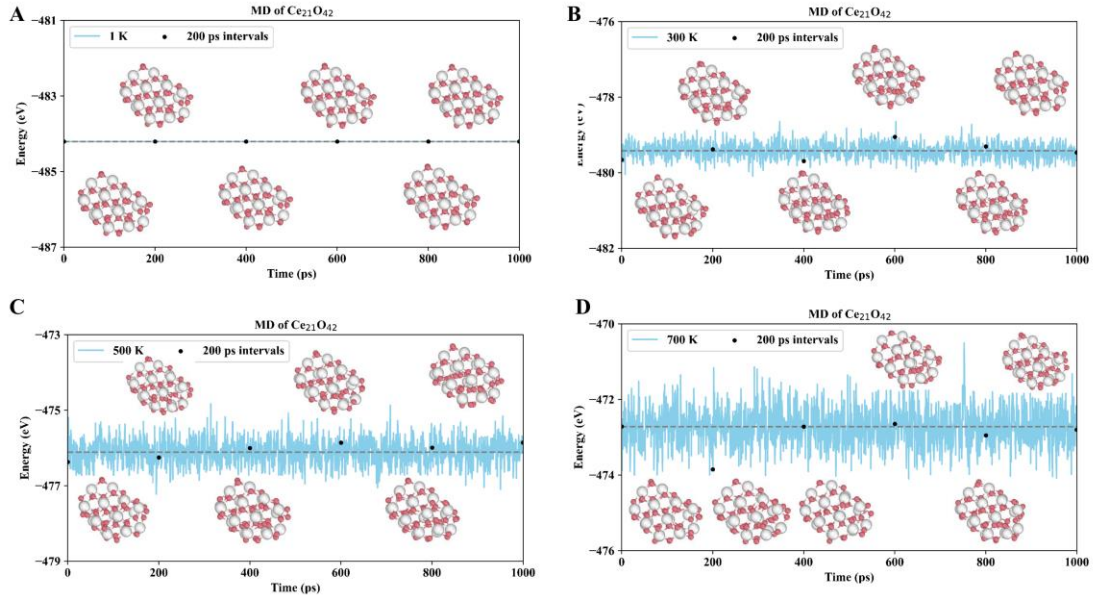


**Supplementary Figure 20.** Molecular dynamics (MD) simulations of the most stable cerium oxide nanocluster $Ce_{21}O_{42}$ at different temperatures, including energies during the simulations and snapshots taken every 200 ps. A: 1 K; B: 300 K; C: 500 K; D: 700 K. Color map: white, Ce atoms; pink, O atoms.

## 4. The NNPMD analysis using unsupervised machine learning algorithms

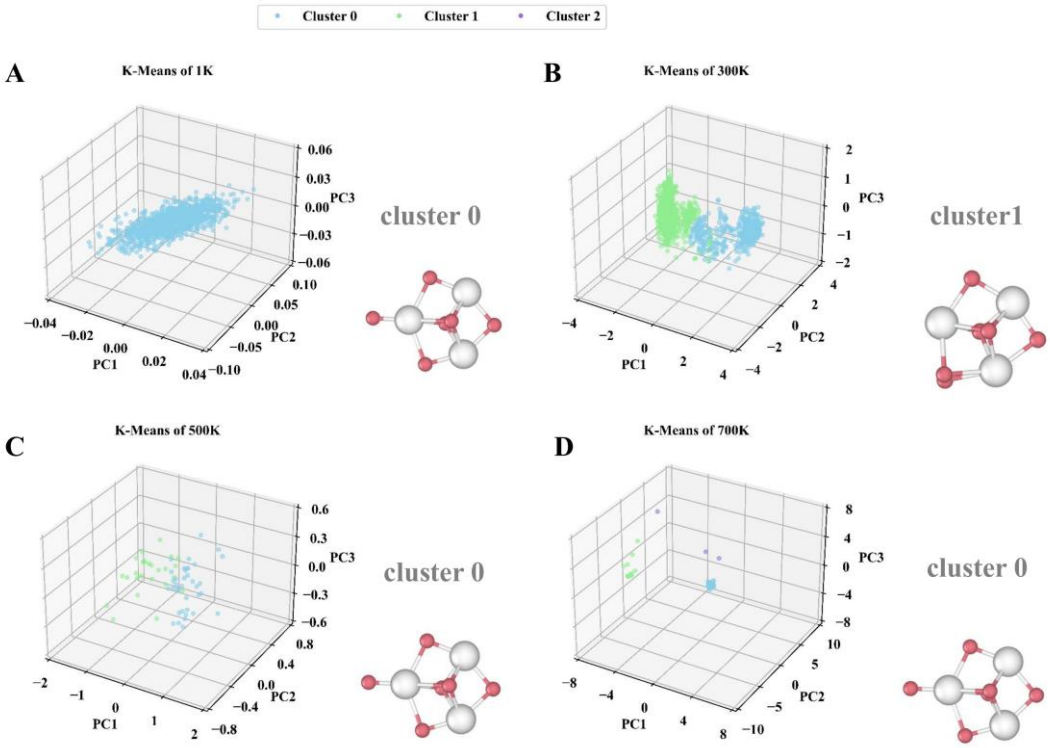


**Supplementary Figure 21.** Visualization of clustered nanocluster $Ce_3O_6$ at different temperatures via PCA dimensionality reduction, along with the representative structure of the largest cluster. A, B, C, and D correspond to 0 K, 300 K, 500 K, and 700 K, respectively. Color map: white, Ce atoms; pink, O atoms.

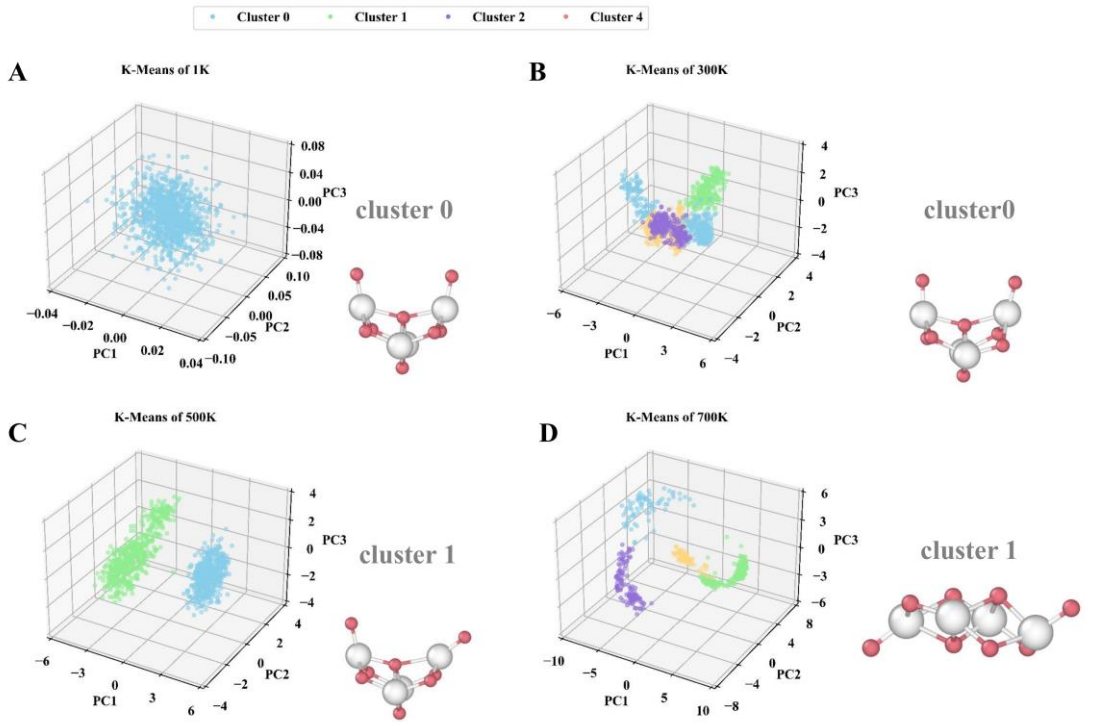


**Supplementary Figure 22.** Visualization of clustered nanocluster $Ce_4O_8$ at different temperatures via PCA dimensionality reduction, along with the representative structure of the largest cluster. A, B, C, and D correspond to 0 K, 300 K, 500 K, and 700 K, respectively. Color map: white, Ce atoms; pink, O atoms

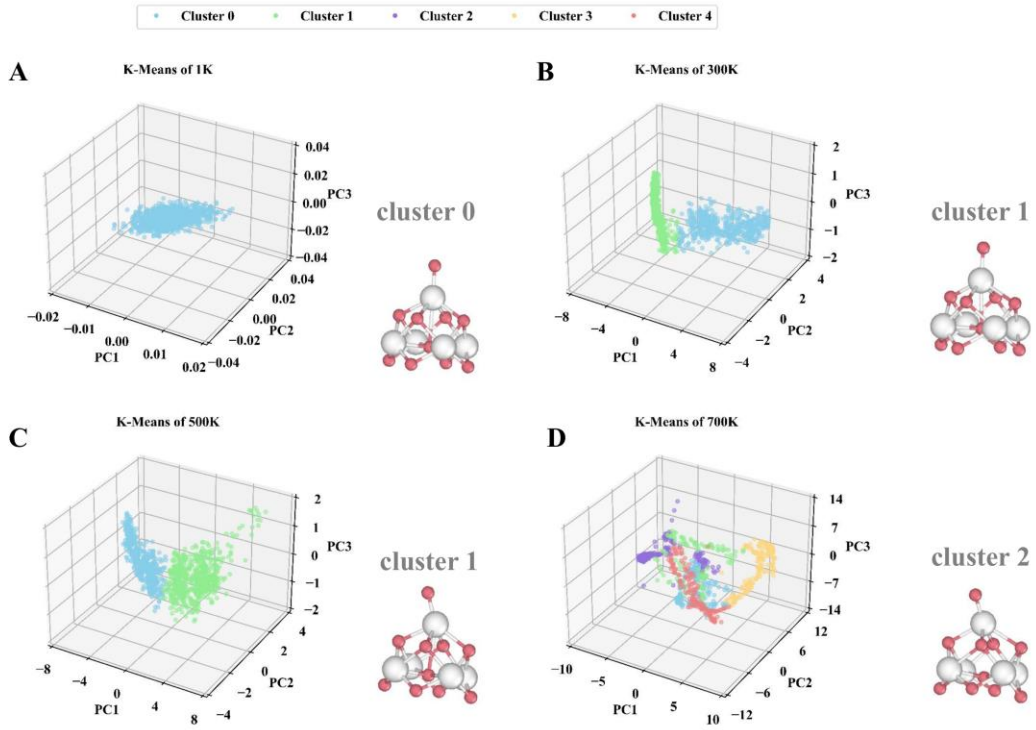

**Supplementary Figure 23.** Visualization of clustered nanocluster $Ce_5O_{10}$ at different temperatures via PCA dimensionality reduction, along with the representative structure of the largest cluster. A, B, C, and D correspond to 0 K, 300 K, 500 K, and 700 K, respectively. Color map: white, Ce atoms; pink, O atoms

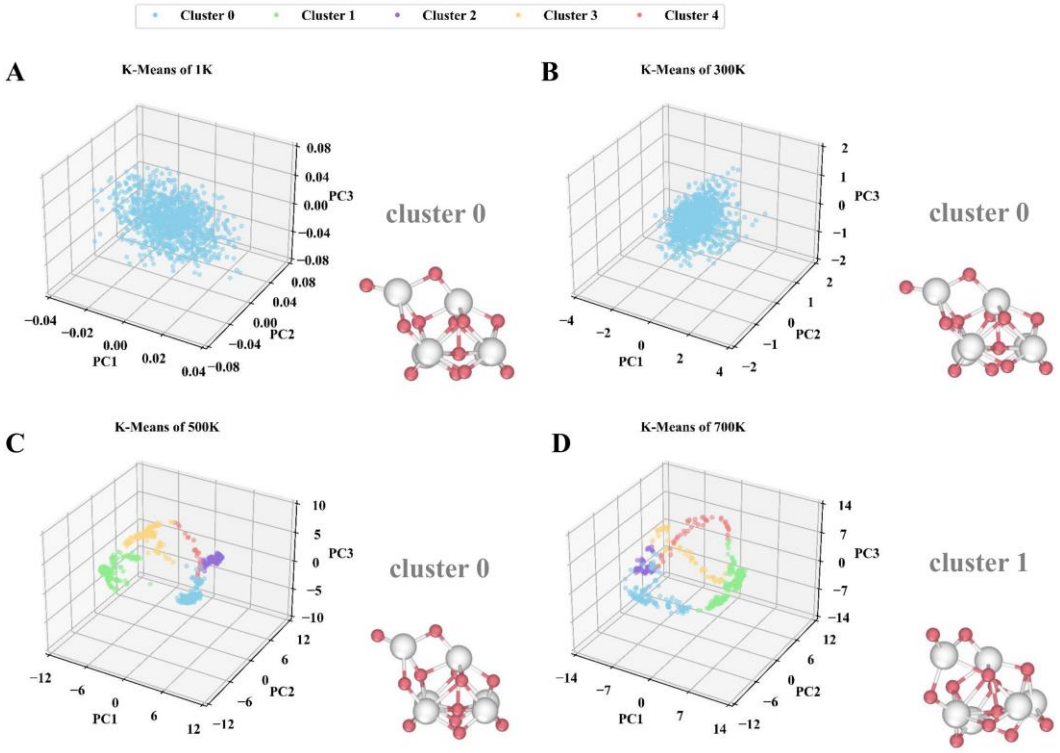


**Supplementary Figure 24.** Visualization of clustered nanocluster $Ce_6O_{12}$ at different temperatures via PCA dimensionality reduction, along with the representative structure of the largest cluster. A, B, C, and D correspond to 0 K, 300 K, 500 K, and 700 K, respectively. Color map: white, Ce atoms; pink, O atoms

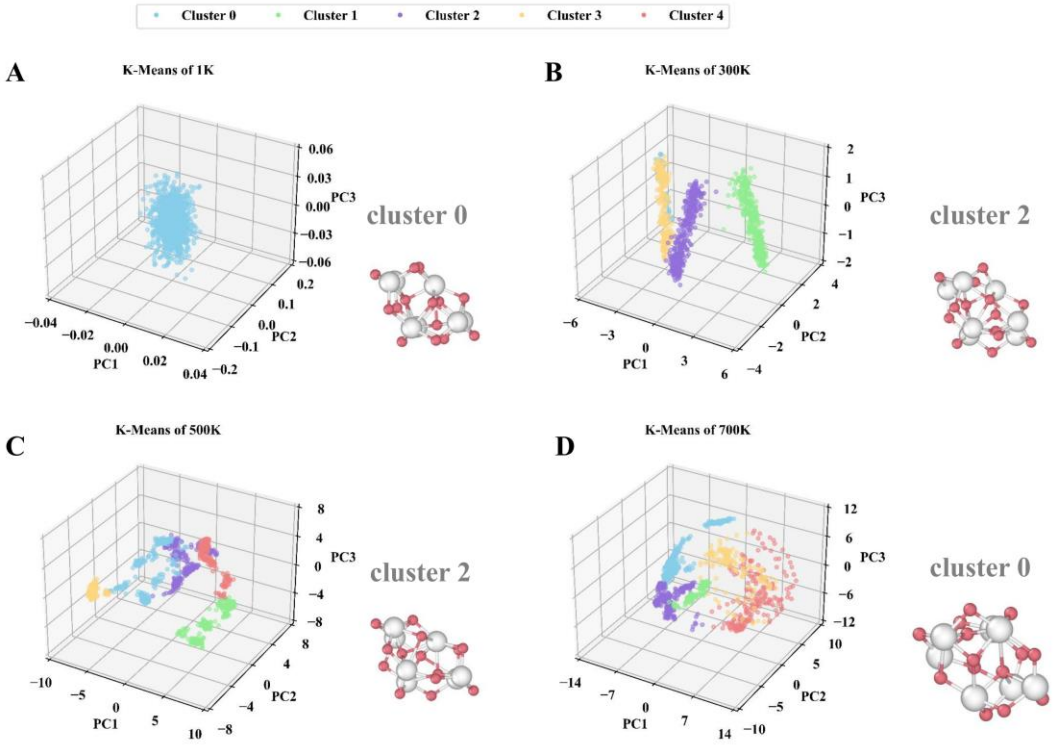


**Supplementary Figure 25.** Visualization of clustered nanocluster $Ce_7O_{14}$ at different temperatures via PCA dimensionality reduction, along with the representative structure of the largest cluster. A, B, C, and D correspond to 0 K, 300 K, 500 K, and 700 K, respectively. Color map: white, Ce atoms; pink, O atoms

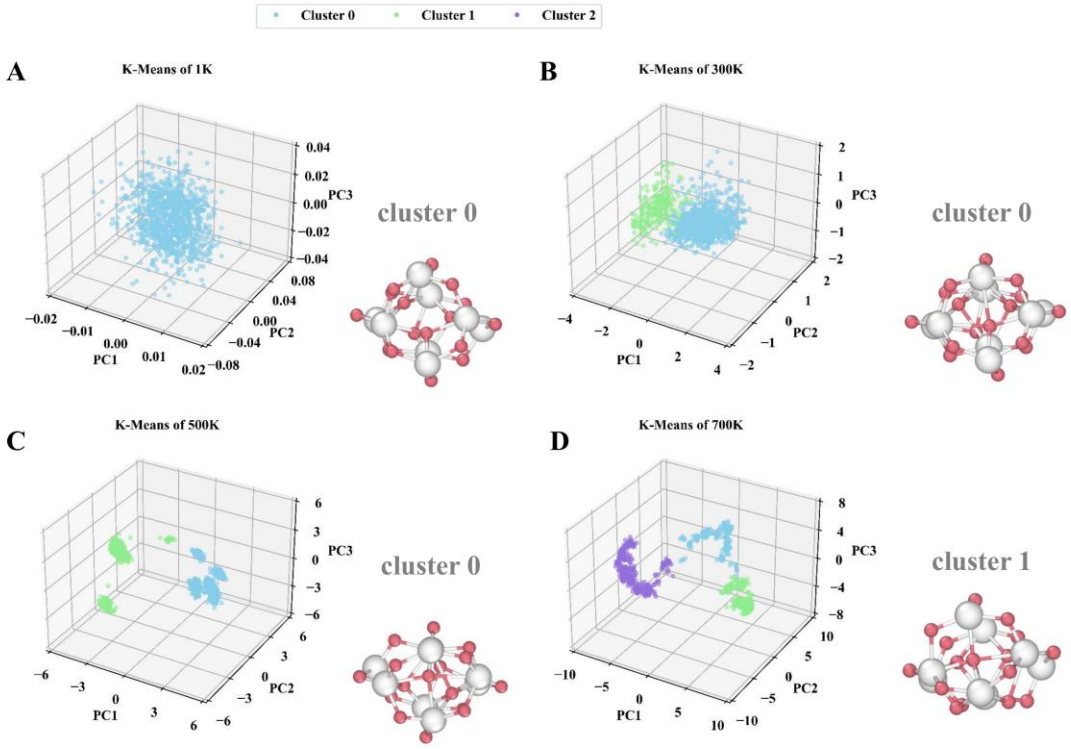


**Supplementary Figure 26.** Visualization of clustered nanocluster $Ce_8O_{16}$ at different temperatures via PCA dimensionality reduction, along with the representative structure of the largest cluster. A, B, C, and D correspond to 0 K, 300 K, 500 K, and 700 K, respectively. Color map: white, Ce atoms; pink, O atoms

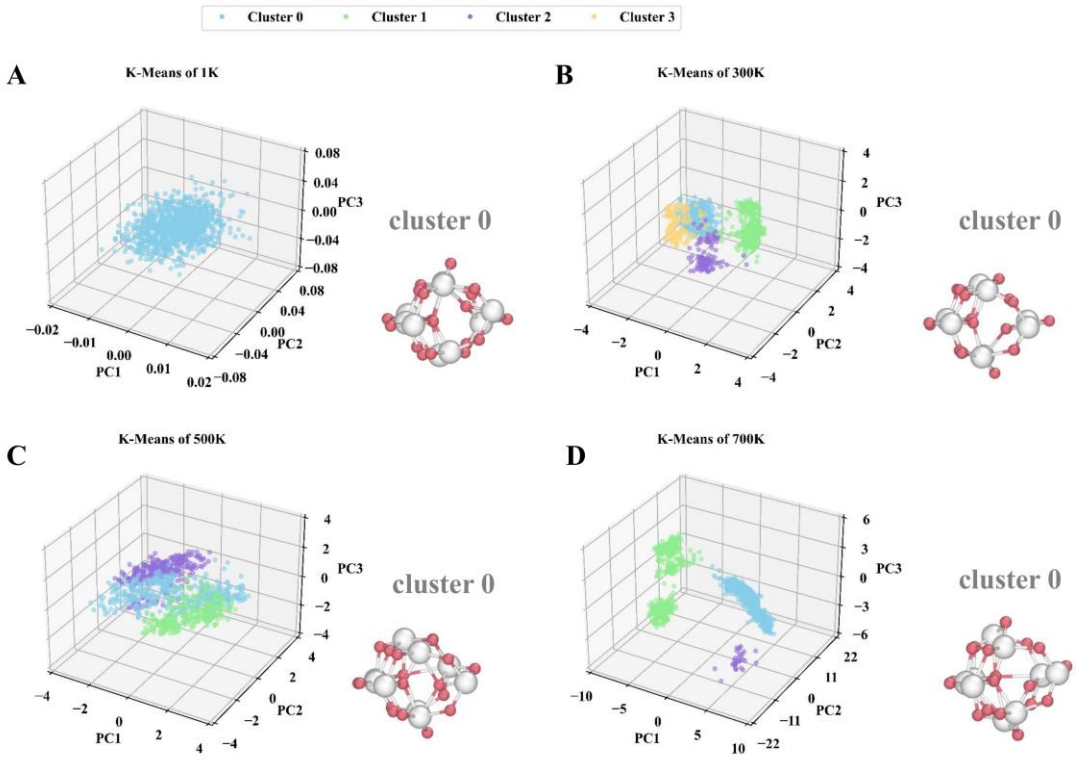


**Supplementary Figure 27.** Visualization of clustered nanocluster $Ce_9O_{18}$ at different temperatures via PCA dimensionality reduction, along with the representative structure of the largest cluster. A, B, C, and D correspond to 0 K, 300 K, 500 K, and 700 K, respectively. Color map: white, Ce atoms; pink, O atoms

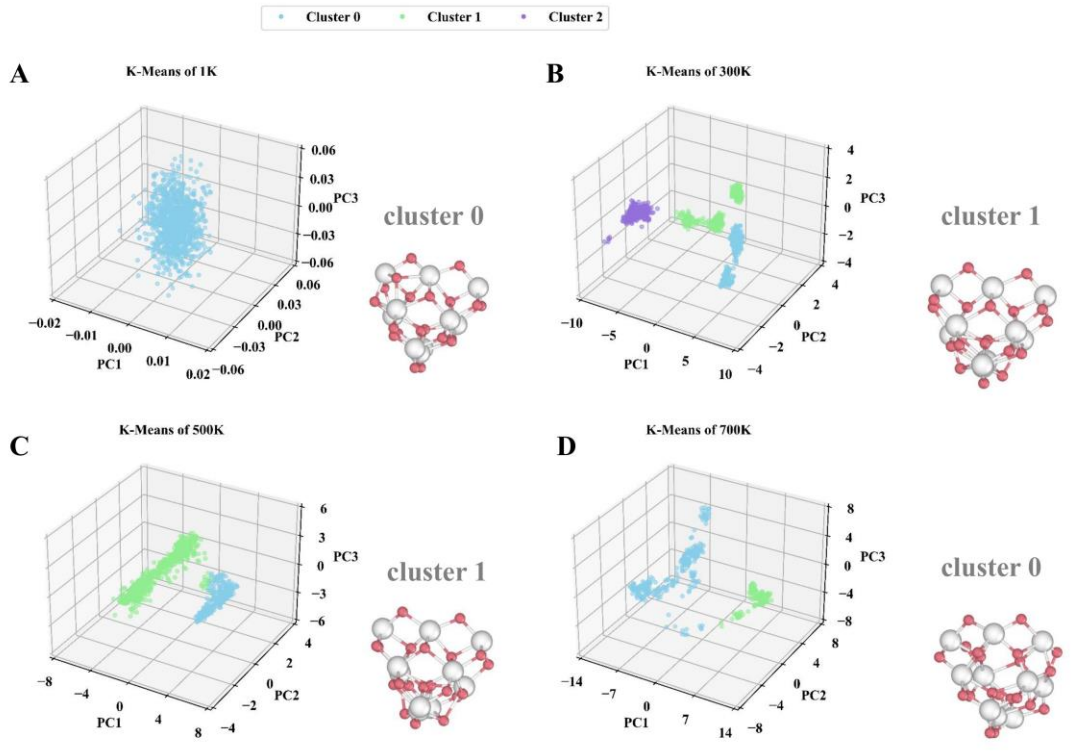

**Supplementary Figure 28.** Visualization of clustered nanocluster $Ce_{10}O_{20}$ at different temperatures via PCA dimensionality reduction, along with the representative structure of the largest cluster. A, B, C, and D correspond to 0 K, 300 K, 500 K, and 700 K, respectively. Color map: white, Ce atoms; pink, O atoms

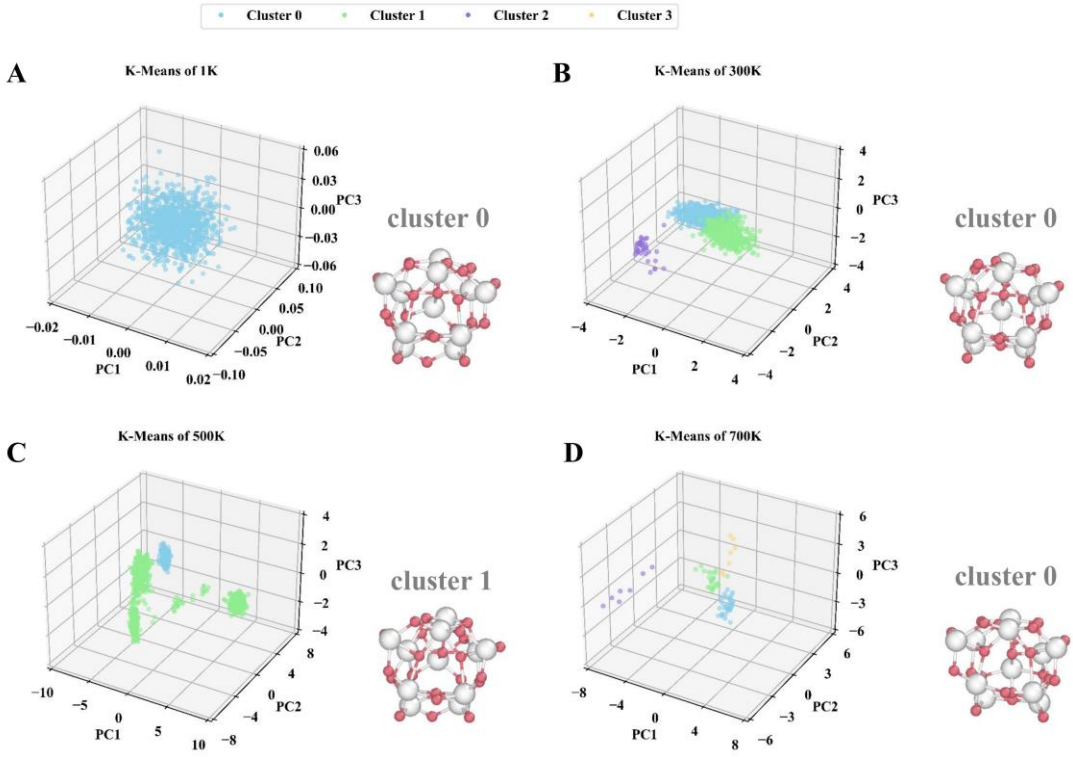


**Supplementary Figure 29.** Visualization of clustered nanocluster $Ce_{11}O_{22}$ at different temperatures via PCA dimensionality reduction, along with the representative structure of the largest cluster. A, B, C, and D correspond to 0 K, 300 K, 500 K, and 700 K, respectively. Color map: white, Ce atoms; pink, O atoms

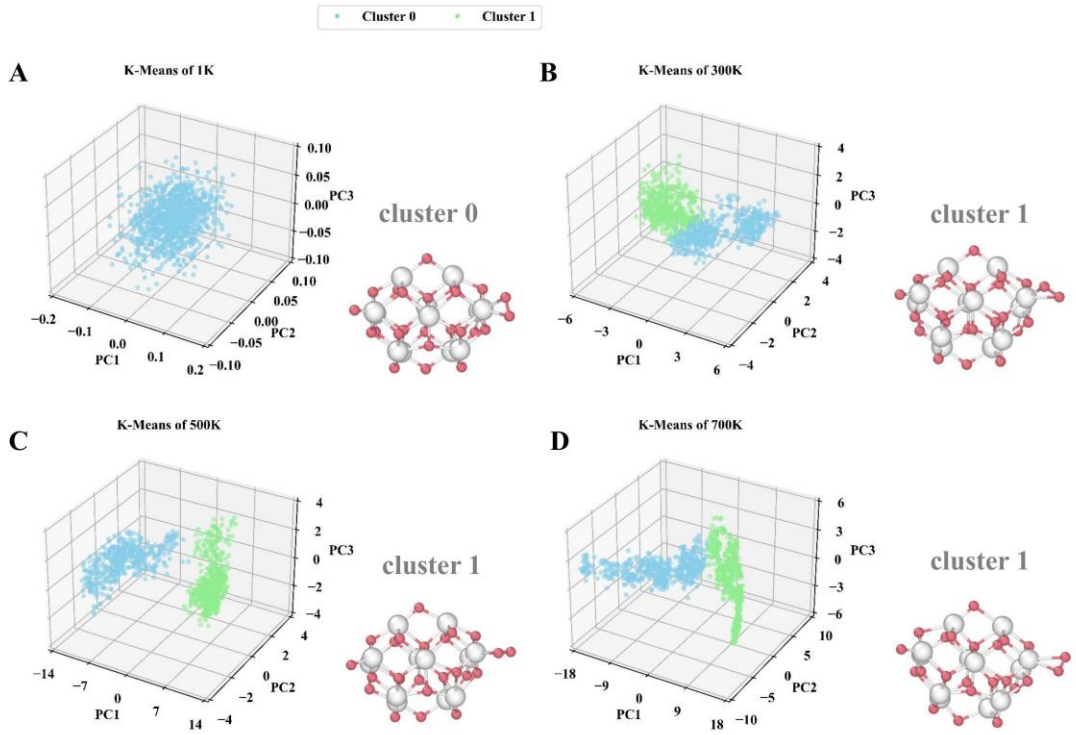


**Supplementary Figure 30.** Visualization of clustered nanocluster $Ce_{12}O_{24}$ at different temperatures via PCA dimensionality reduction, along with the representative structure of the largest cluster. A, B, C, and D correspond to 0 K, 300 K, 500 K, and 700 K, respectively. Color map: white, Ce atoms; pink, O atoms

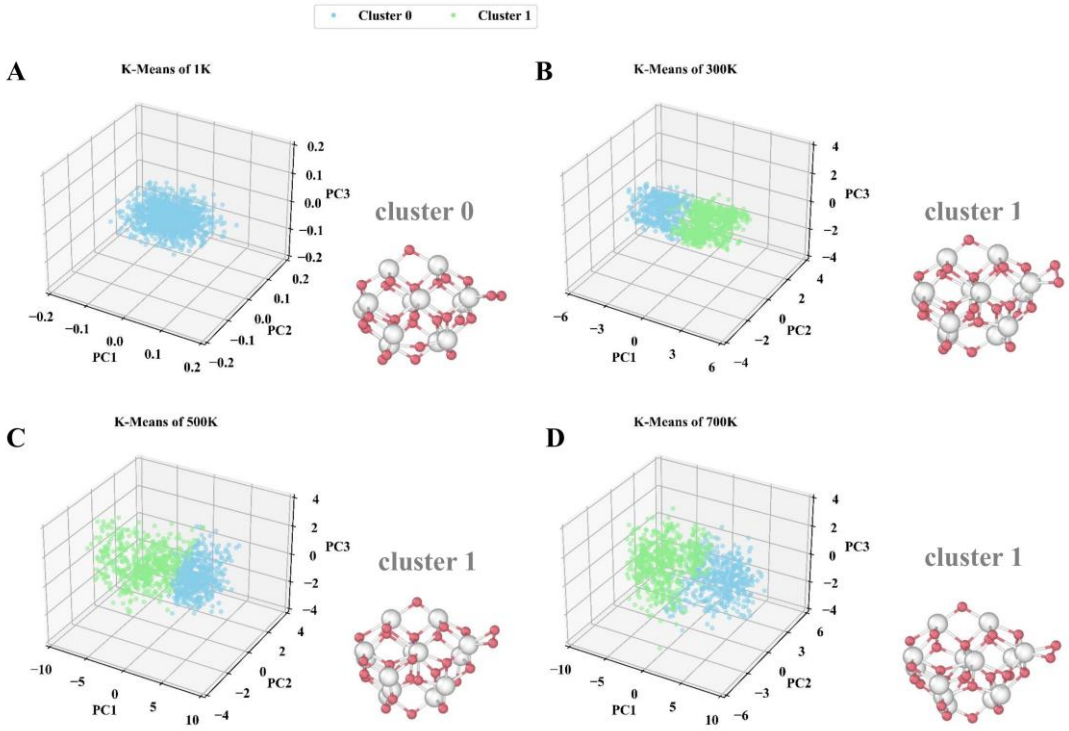

**Supplementary Figure 31.** Visualization of clustered nanocluster $Ce_{13}O_{26}$ at different temperatures via PCA dimensionality reduction, along with the representative structure of the largest cluster. A, B, C, and D correspond to 0 K, 300 K, 500 K, and 700 K, respectively. Color map: white, Ce atoms; pink, O atoms

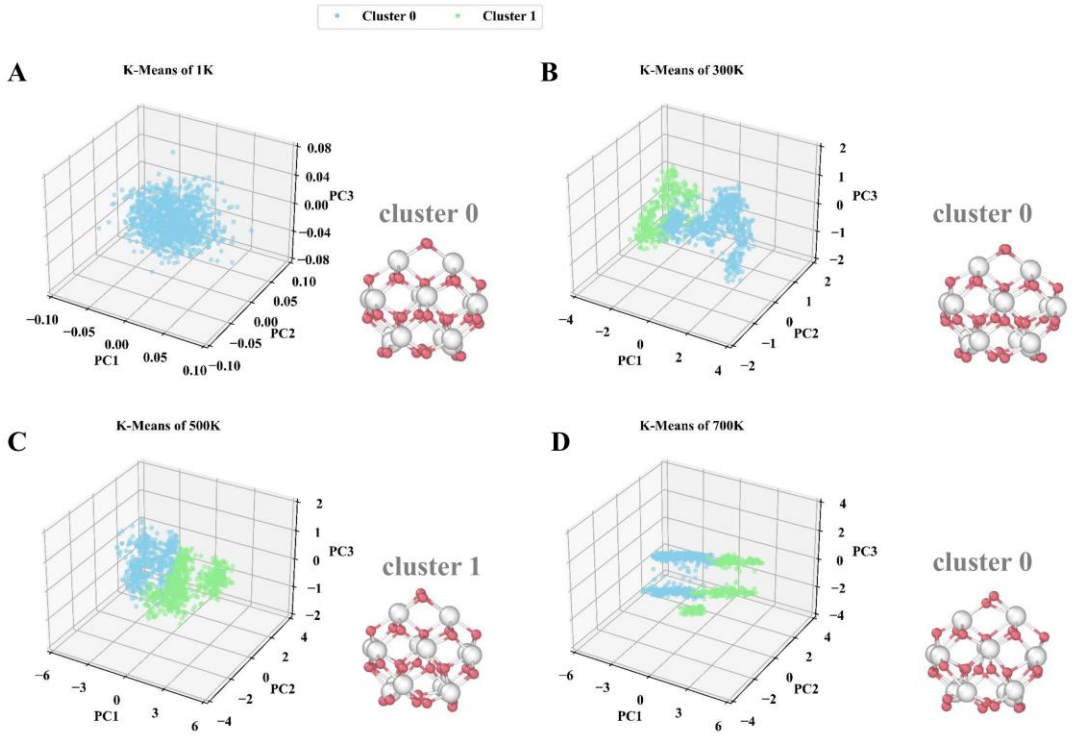


**Supplementary Figure 32.** Visualization of clustered nanocluster $Ce_{14}O_{28}$ at different temperatures via PCA dimensionality reduction, along with the representative structure of the largest cluster. A, B, C, and D correspond to 0 K, 300 K, 500 K, and 700 K, respectively. Color map: white, Ce atoms; pink, O atoms

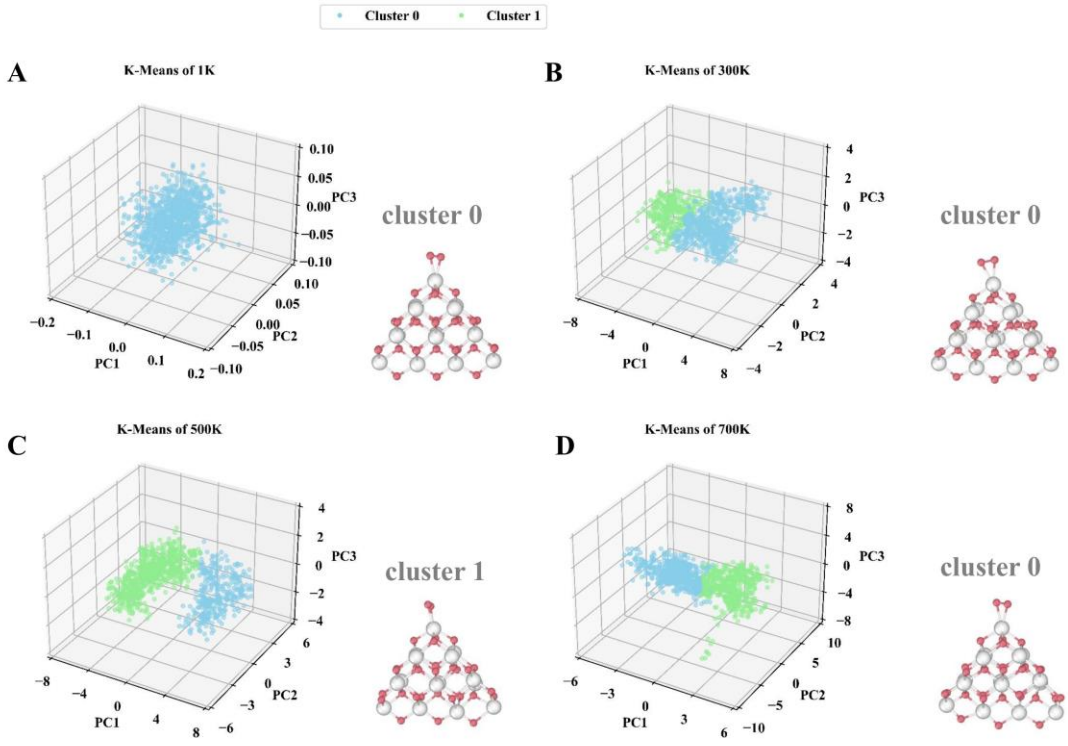


**Supplementary Figure 33.** Visualization of clustered nanocluster $Ce_{15}O_{30}$ at different temperatures via PCA dimensionality reduction, along with the representative structure of the largest cluster. A, B, C, and D correspond to 0 K, 300 K, 500 K, and 700 K, respectively. Color map: white, Ce atoms; pink, O atoms

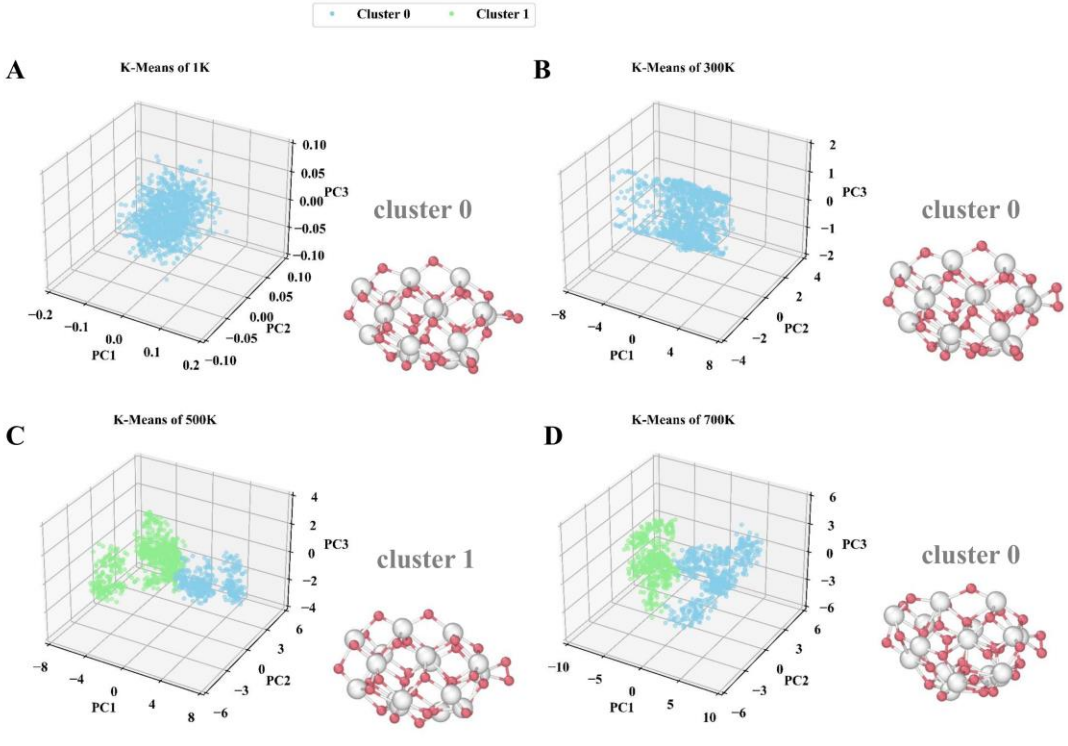

**Supplementary Figure 34.** Visualization of clustered nanocluster $Ce_{16}O_{32}$ at different temperatures via PCA dimensionality reduction, along with the representative structure of the largest cluster. A, B, C, and D correspond to 0 K, 300 K, 500 K, and 700 K, respectively. Color map: white, Ce atoms; pink, O atoms

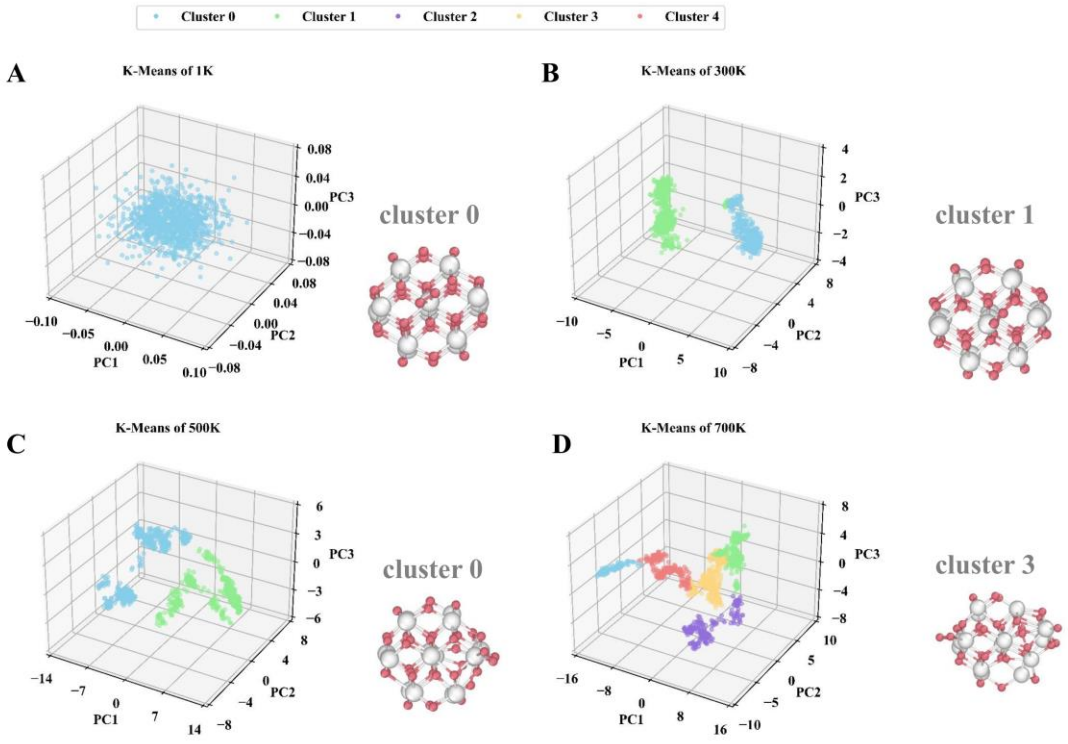


**Supplementary Figure 35.** Visualization of clustered nanocluster $Ce_{17}O_{34}$ at different temperatures via PCA dimensionality reduction, along with the representative structure of the largest cluster. A, B, C, and D correspond to 0 K, 300 K, 500 K, and 700 K, respectively. Color map: white, Ce atoms; pink, O atoms

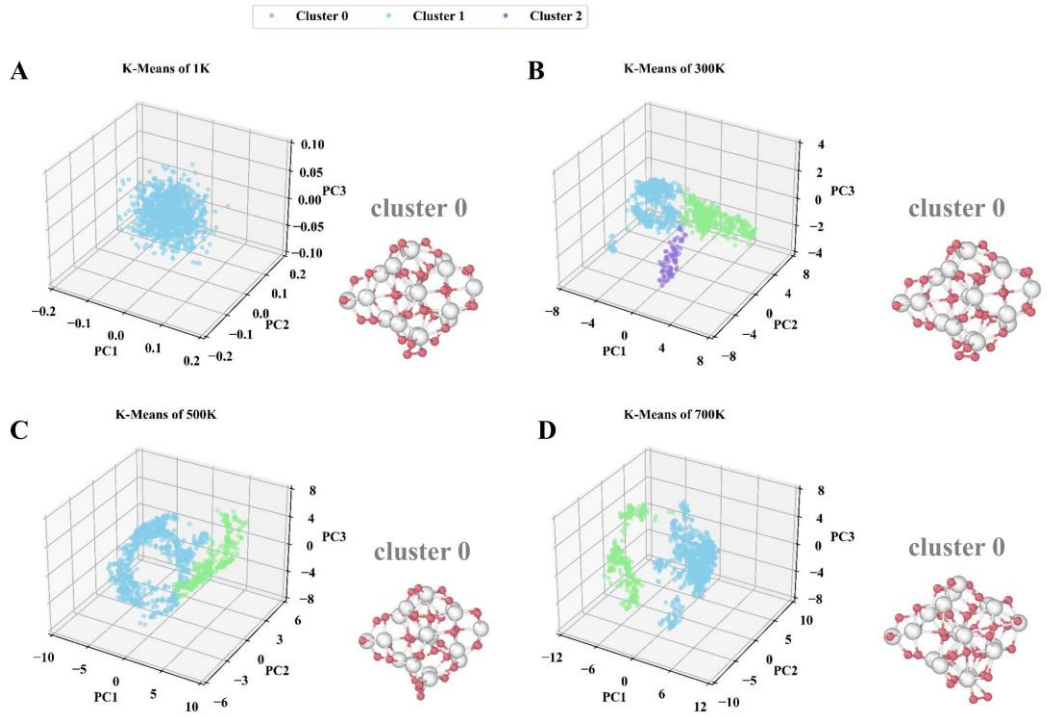


**Supplementary Figure 36.** Visualization of clustered nanocluster $Ce_{18}O_{36}$ at different temperatures via PCA dimensionality reduction, along with the representative structure of the largest cluster. A, B, C, and D correspond to 0 K, 300 K, 500 K, and 700 K, respectively. Color map: white, Ce atoms; pink, O atoms

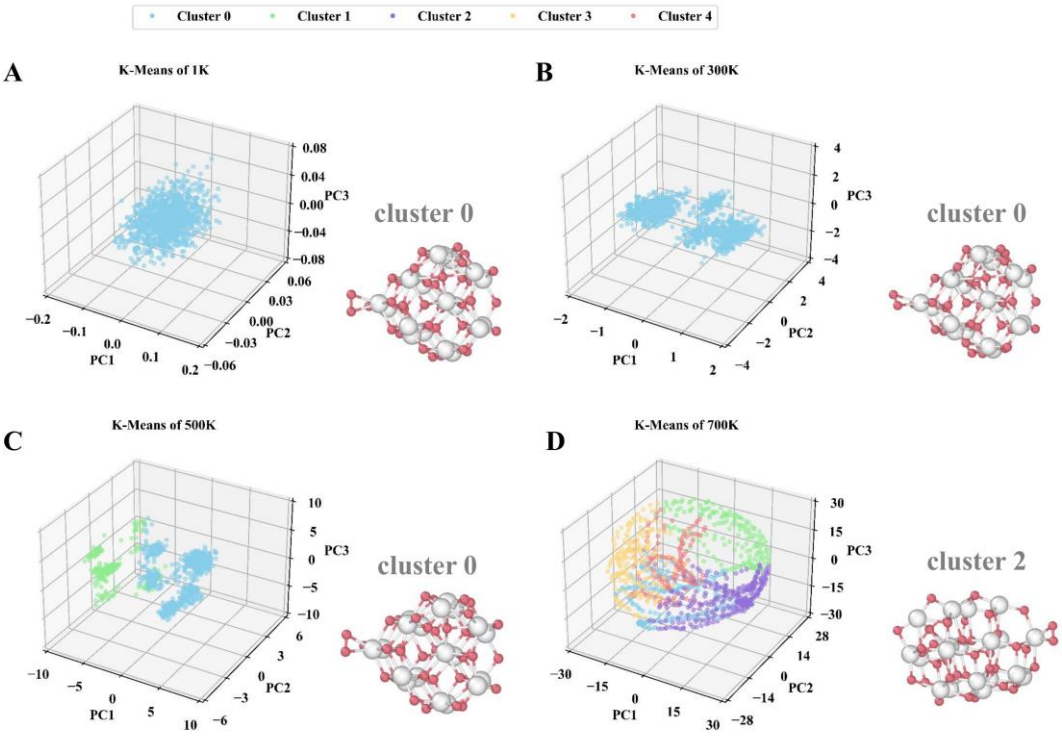

**Supplementary Figure 37.** Visualization of clustered nanocluster $Ce_{19}O_{38}$ at different temperatures via PCA dimensionality reduction, along with the representative structure of the largest cluster. A, B, C, and D correspond to 0 K, 300 K, 500 K, and 700 K, respectively. Color map: white, Ce atoms; pink, O atoms.

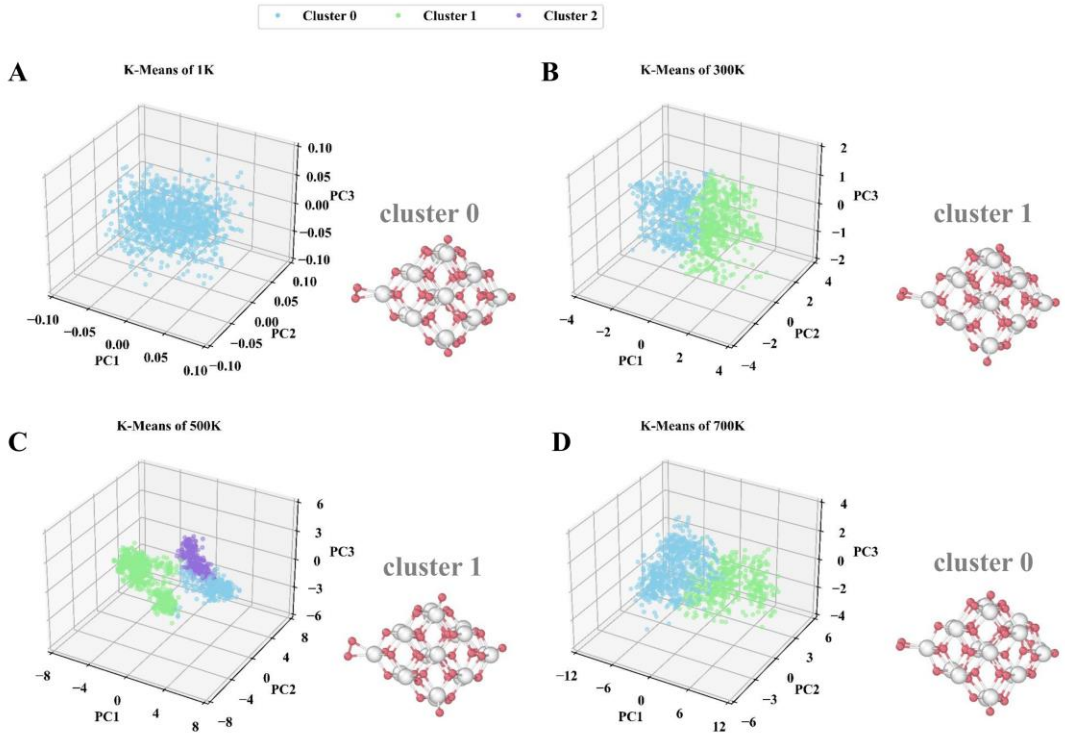


**Supplementary Figure 38.** Visualization of clustered nanocluster $Ce_{20}O_{40}$ at different temperatures via PCA dimensionality reduction, along with the representative structure of the largest cluster. A, B, C, and D correspond to 0 K, 300 K, 500 K, and 700 K, respectively. Color map: white, Ce atoms; pink, O atoms

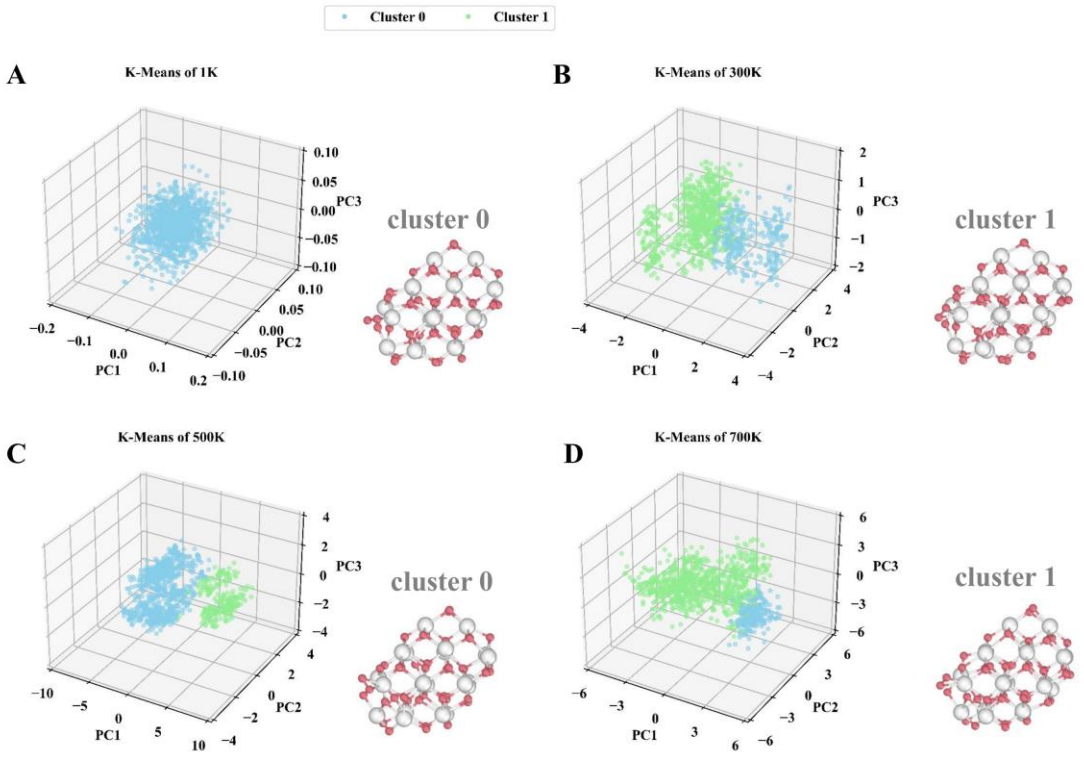


**Supplementary Figure 39.** Visualization of clustered nanocluster $Ce_{21}O_{42}$ at different temperatures via PCA dimensionality reduction, along with the representative structure of the largest cluster. A, B, C, and D correspond to 0 K, 300 K, 500 K, and 700 K, respectively. Color map: white, Ce atoms; pink, O atoms

**Supplementary Table 3. Average energy, RMSD, and number of each largest cluster after clustering**

| | 1 K | | | | 300 K | | | |
|---|---|---|---|---|---|---|---|---|
| | Avg Etot | Avg Ep | Avg RMSD | Num | Avg Etot | Avg Ep | Avg RMSD | Num |
| Ce3O6 | -64.18 | -64.18 | 0.087 | 1001 | -64.079 | -64.129 | 1.71 | 553 |
| Ce4O8 | -87.026 | -87.026 | 0.033 | 1001 | -86.899 | -86.963 | 0.352 | 328 |
| Ce5O10 | -110.42 | -110.421 | 0.054 | 1001 | -110.231 | -110.326 | 0.252 | 509 |
| Ce6O12 | -133.289 | -133.289 | 0.036 | 1001 | -133.1 | -133.195 | 0.328 | 718 |
| Ce7O14 | -156.521 | -156.522 | 0.043 | 1001 | -156.328 | -156.436 | 0.47 | 397 |
| Ce8O16 | -179.914 | -179.915 | 0.088 | 1001 | -179.711 | -179.836 | 0.354 | 786 |
| Ce9O18 | -203.065 | -203.065 | 0.043 | 1001 | -202.769 | -202.925 | 0.557 | 391 |

| | | | | | | | | |
|---|---|---|---|---|---|---|---|---|
| Ce10O20 | -226.348 | -226.349 | 0.028 | 1001 | -226.095 | -226.222 | 0.785 | 290 |
| Ce11O22 | -249.096 | -249.097 | 0.05 | 1001 | -248.768 | -248.933 | 0.445 | 553 |
| Ce12O24 | -272.996 | -272.997 | 0.08 | 1001 | -272.528 | -272.76 | 0.57 | 509 |
| Ce13O26 | -296.215 | -296.216 | 0.039 | 1001 | -295.736 | -295.98 | 0.453 | 579 |
| Ce14O28 | -319.956 | -319.957 | 0.05 | 1001 | -319.522 | -319.742 | 0.221 | 635 |
| Ce15O30 | -343.78 | -343.781 | 0.032 | 1001 | -343.267 | -343.524 | 0.708 | 652 |
| Ce16O32 | -366.148 | -366.149 | 0.047 | 1001 | -365.519 | -365.833 | 0.333 | 545 |
| Ce17O34 | -388.843 | -388.844 | 0.142 | 1001 | -388.336 | -388.589 | 0.359 | 607 |
| Ce18O36 | -412.861 | -412.862 | 0.078 | 1001 | -412.129 | -412.496 | 0.344 | 534 |
| Ce19O38 | -436.686 | -436.688 | 0.03 | 1001 | -436.051 | -436.369 | 0.231 | 449 |
| Ce20O40 | -461.273 | -461.275 | 0.088 | 1001 | -460.63 | -460.952 | 0.451 | 508 |
| Ce21O41 | -484.217 | -484.219 | 0.041 | 1001 | -483.538 | -483.878 | 0.319 | 721 |

| | 500 K | | | | 700 K | | | |
|---|---|---|---|---|---|---|---|---|
| | Avg Etot | Avg Ep | Avg RMSD | Num | Avg Etot | Avg Ep | Avg RMSD | Num |
| Ce3O6 | -64.178 | -64.179 | 0.138 | 37 | -64.176 | -64.178 | 0.229 | 76 |
| Ce4O8 | -86.794 | -86.911 | 0.694 | 532 | -86.77 | -86.899 | 2.128 | 188 |
| Ce5O10 | -110.1 | -110.259 | 0.664 | 552 | -110.071 | -110.245 | 0.832 | 381 |
| Ce6O12 | -132.987 | -133.138 | 0.615 | 481 | -132.946 | -133.116 | 1.19 | 244 |
| Ce7O14 | -156.198 | -156.37 | 0.821 | 251 | -155.988 | -156.264 | 1.791 | 306 |
| Ce8O16 | -179.578 | -179.769 | 0.48 | 602 | -179.233 | -179.597 | 1.577 | 385 |
| Ce9O18 | -202.573 | -202.825 | 0.721 | 451 | -202.293 | -202.681 | 0.669 | 576 |
| Ce10O20 | -225.725 | -226.037 | 1.195 | 707 | -225.768 | -226.058 | 2.357 | 270 |
| Ce11O22 | -248.453 | -248.775 | 0.634 | 474 | -248.523 | -248.815 | 1.156 | 32 |
| Ce12O24 | -272.232 | -272.613 | 0.459 | 566 | -271.917 | -272.467 | 2.193 | 507 |
| Ce13O26 | -295.383 | -295.801 | 0.475 | 532 | -295.281 | -295.855 | 0.568 | 544 |
| Ce14O28 | -319.066 | -319.514 | 0.459 | 569 | -319.057 | -319.548 | 0.333 | 664 |
| Ce15O30 | -342.827 | -343.305 | 0.569 | 671 | -342.629 | -343.206 | 0.569 | 551 |

| | | | | | | | | |
|---|---|---|---|---|---|---|---|---|
| Ce16O32 | -365.209 | -365.681 | 0.437 | 660 | -365.034 | -365.592 | 0.922 | 540 |
| Ce17O34 | -388.037 | -388.439 | 1.147 | 565 | -387.576 | -388.257 | 2.229 | 282 |
| Ce18O36 | -411.862 | -412.359 | 0.853 | 427 | -411.299 | -412.081 | 0.87 | 763 |
| Ce19O38 | -435.761 | -436.274 | 0.402 | 770 | -435.303 | -436.042 | 3.288 | 291 |
| Ce20O40 | -460.339 | -460.822 | 0.452 | 539 | -459.786 | -460.643 | 0.581 | 587 |
| Ce21O41 | -483.103 | -483.66 | 0.45 | 779 | -482.474 | -483.36 | 0.534 | 819 |

**References**


1. Behler, J.; Parrinello, M. Generalized Neural-Network Representation of High-Dimensional Potential-Energy Surfaces. *Physical Review Letters*. **2007**, *98*, 146401. DOI: 10.1103/PhysRevLett.98.146401

2. Behler, J. Atom-centered symmetry functions for constructing high-dimensional neural network potentials. *The Journal of Chemical Physics*. **2011**, *134*, 074106. DOI: 10.1063/1.3553717

3. Singraber, A.; Morawietz, T.; Behler, J.; et al. Parallel Multistream Training of High-Dimensional Neural Network Potentials. *Journal of Chemical Theory and Computation*. **2019**, *15*, 3075-3092. DOI: 10.1021/acs.jctc.8b01092